

AN ABSTRACT OF THE THESIS OF

LAWRENCE EDWARD WILES for the MASTER OF SCIENCE

(Name of student)

(Degree)

in Mechanical Engineering presented on

(Major)

March 25 1974

(Date)

Title: AN EXPERIMENTAL INVESTIGATION OF LAMINAR

NATURAL CONVECTION WITH A UNIFORMLY HEATED

VERTICAL CYLINDER IN MERCURY

Redacted for privacy

Abstract approved: _____

Dr. J. R. Welty

An experimental investigation of laminar natural convection heat transfer from a uniformly heated vertical circular cylinder immersed in an effectively infinite pool of mercury has been performed. Each of the three heated sections used in the study was 3.85 inches high. Diameters of the heated sections were 0.590, 1.355 and 2.108 inches.

For each cylinder a correlation was developed for the local Nusselt number as a function of local modified Grashof number. Local parameters were based on the axial distance from the leading edge of the cylinder. A single equation incorporating the diameter-to-length ratio was formulated that satisfied the data quite well for all three cylinders. The data were extrapolated graphically to the case of zero curvature; i. e., a flat plate, and the result was found

to agree quite closely with other work, both analytical and experimental.

The influence of curvature upon the heat transfer was found to be small but significant. It was established that the effective thermal resistance through the boundary layer is less for a cylinder of finite curvature than for a flat plate. Consequently, a cylinder will exhibit a larger Nusselt number than will a flat plate.

An Experimental Investigation of Laminar Natural Convection
With a Uniformly Heated Vertical Cylinder in Mercury

by

Lawrence Edward Wiles

A THESIS

submitted to

Oregon State University

in partial fulfillment of
the requirements for the
degree of

Master of Science

June 1974

APPROVED:

Redacted for privacy

Professor of Mechanical Engineering
in charge of major

Redacted for privacy

Head of Department of Mechanical Engineering

Redacted for privacy

Dean of Graduate School

Date thesis is presented

March 25, 1974

Typed by Ilene Anderton for Lawrence Edward Wiles

TABLE OF CONTENTS

<u>Chapter</u>	<u>Page</u>
I. INTRODUCTION	1
II. LITERATURE REVIEW	4
2.1 Flat Plates	4
2.2 Circular Cylinders	11
III. EXPERIMENTAL DESIGN	16
3.1 Apparatus	16
3.1.1 Construction of the Heated Cylinders	16
3.1.2 Basic Test Section	20
3.1.3 Additional Equipment	23
3.2 Procedure	24
3.3 Sources of Error	27
IV. HEAT TRANSFER RESULTS	35
V. DIMENSIONLESS TEMPERATURE	51
VI. CONCLUSIONS	59
BIBLIOGRAPHY	61
APPENDIX A.1	64
APPENDIX A.2	68

LIST OF TABLES

<u>Table</u>	<u>Page</u>
T2. 1. Heat transfer results of Ostrach (4) $\text{Nu}_L = (4/3)f(\text{Pr}) \text{Gr}_L^{0.25}$	7
T3. 1. Nu_x vs. Gr_x^* as calculated from regression equations E4. 2.	30
T4. 1. Values of Nu_x at $\frac{L}{D} = 0$ for values of Gr_x^* .	42
T4. 2. Summary of heat transfer correlations for uniform flux flat plates.	48

LIST OF FIGURES

<u>Figure</u>	<u>Page</u>
F3. 1. The three completed cylinders.	17
F3. 2. Heaters before assembly.	17
F3. 3. Circuit pattern of heaters with dimensions.	19
F3. 4. Schematic of basic test section.	21
F3. 5. Basic test section.	22
F3. 6. Overall view of apparatus.	22
F4. 1. Heat transfer data; cylinder 1.	37
F4. 2. Heat transfer data; cylinder 2.	38
F4. 3. Heat transfer data; cylinder 3.	39
F4. 4. Heat transfer data; all cylinders.	41
F4. 5. Plot to determine Nu_x at $\frac{L}{D} = 0$ for various Gr_x^* .	43
F4. 6. Plot of intercepts to determine equation of extrapolation to flat plate.	44
F4. 7. Plot of results for uniformly heated vertical flat plates.	49
F4. 8. Plot of regression equations for cylinders 1, 2, and 3 compared to equation E4. 5 and the results of Julian (11).	50
F5. 1. Dimensionless temperature; cylinder 1.	53
F5. 2. Dimensionless temperature; cylinder 2.	54
F5. 3. Dimensionless temperature; cylinder 3.	55

NOMENCLATURE

<u>Notation</u>	<u>Description</u>
Cylinder 1	: refers to cylinder of diameter 0.590"
Cylinder 2	: refers to cylinder of diameter 1.355"
Cylinder 3	: refers to cylinder of diameter 2.108"
C	: constant
C'	: constant
n	: exponent of Grashof number
n_i	: exponent to which variable i appears in C'
E_i	: error in variable i
j	: number of variables involved in summation of errors
g	: acceleration of gravity
k	: thermal conductivity
ν	: kinematic viscosity
β	: coefficient of thermal expansion; $= 0.000101/^\circ\text{F}$
q	: surface heat flux
x	: distance from leading edge of heated section
L	: length of heated section : length over which heat transfer occurs
D	: diameter of cylinder
r	: radial distance from heated surface
Pr	: Prandtl number

- $f(\text{Pr})$: function of Prandtl number
- S : all terms in modified Grashof number except length variable, $= \left(\frac{\beta g}{\nu^2 k}\right) \cdot q$
- Gr' : Grashof number dependent on $\left(\frac{dT}{dx}\right)_o$
- ^+Gr : Grashof number $= \left(\frac{\beta g}{\nu^2}\right) \cdot L^3 \cdot \Delta T$
- $^+\text{Gr}^*$: modified Grashof number $= \left(\frac{\beta g}{\nu^2 k}\right) \cdot q \cdot L^4$; evaluated at $T_r = 0.7 T_w + 0.3 T_\infty$
- ^+Ra : Rayleigh number $= \text{Gr} \cdot \text{Pr}$
- $^+\text{Ra}^*$: modified Rayleigh number $= \text{Gr}^* \cdot \text{Pr}$
- h_x : local film coefficient
- h_m : averaged film coefficient
- ^+Nu : Nusselt number $= \frac{hL}{k} = \frac{qL}{k\Delta T}$; evaluated at T_w
- T : local fluid temperature
- T_∞ : ambient fluid temperature
- T_w : temperature of heated surface
- ΔT : $T_w - T_\infty$
- $\overline{\Delta T}$: average of ΔT over surface; $\overline{T_w - T_\infty}$
- $\left(\frac{dT}{dx}\right)_o$: slope of surface temperature increase in the x-direction at $x = 0$
- $\left(\frac{dT}{dr}\right)_o$: slope of radial temperature gradient at surface of cylinder

⁺The dimensionless groups may appear in the text with various subscripts referring to the dimension upon which the group is based.

ϕ : $(T - T_{\infty}) / (T_w - T_{\infty})$

θ : dimensionless temperature defined by equation E5.1;

evaluated at $T_r = 0.7 T_w + 0.3 T_{\infty}$

η : dimensionless temperature defined by equation E5.2;

evaluated at $T_r = 0.7 T_w + 0.3 T_{\infty}$

$f(\eta)$: function of η

AN EXPERIMENTAL INVESTIGATION OF LAMINAR NATURAL CONVECTION WITH A UNIFORMLY HEATED VERTICAL CYLINDER IN MERCURY

I. INTRODUCTION

Motivation for the research described in this report was provided by the needs of the United States Atomic Energy Commission involved with reactor research and by the desire to expand current knowledge of the natural convection phenomenon.

The nuclear power plants of the future will be of the liquid metal fast breeder reactor (LMFBR) type. The coolant medium in the reactor core will be a liquid metal and, therefore, will have a very low Prandtl number. In the event of a pump failure involving the coolant the only mode of heat transfer from the core will be that of natural convection. Safe operation under such conditions requires knowledge of the total heat transfer, flow rates, and temperature extremes that can be expected to occur.

The problem of natural convection from certain vertical geometries has been studied analytically and solutions to the governing equations of momentum and energy are presented in the literature for a range of Prandtl numbers including those characteristic of the liquid metals. The validity of applying these results to low Prandtl number fluids is in question, however, because of the assumptions

involved in reducing the governing equations to a simplified, and solvable, form. To increase the present understanding of the heat transfer phenomenon in the low Prandtl number range, an experimental effort is certainly necessary and justified.

Until recently there has been very little comprehensive experimental effort given to the problem of natural convection from vertical surfaces to liquid metals. As a result of efforts at Oregon State University and elsewhere, heat transfer from the vertical flat plate has been studied and documented for the case of uniform wall heat flux. Studies of the heat transfer from uniformly heated, opposing walls of an open, vertical channel and studies of transition from laminar to turbulent flow in a channel have been or are being performed at Oregon State University.

The next logical step towards modeling the geometry of the reactor was to consider the single vertical cylinder with uniform surface heat flux. The initial study involved the laminar flow regime only. The basic goal of this work was to establish relationships between the pertinent heat transfer variables.

A priori, one would expect to find a relation for the local Nusselt number as a function of local modified Grashof number and the diameter of the vertical cylinder. Appearance of the diameter in the results will indicate the effect of curvature upon the heat transfer. This information will be useful in its own right but will

also be a fundamental building block for evaluation of the results attained from future studies involving more complicated geometries.

It is at first assumed that the heat transfer results for a flat plate will differ from the results for a cylinder of some finite diameter due to the effects of curvature. In the case of the vertical circular cylinder, heat transferred away from the surface and conducted through the boundary layer encounters an ever increasing heat transfer area. This is in contrast to the flat plate where the heat transfer area remains constant at increasing distances from the surface. Since thermal resistance is inversely proportional to the heat transfer area through the boundary layer it is apparent that the thermal resistance from the surface of a cylinder to the ambient fluid is less than that for a flat plate. As a consequence, a cylinder of finite radius will experience a smaller temperature difference between its surface and the ambient fluid than will a flat plate when subjected to the same surface heat flux. This would imply that the cylinder Nusselt number should be larger than the Nusselt number for a flat plate under identical conditions. Also, it would be expected that the Nusselt number would continue to increase with increasing curvature.

II. LITERATURE REVIEW

2.1 Flat Plates

The study of natural convection flows from vertical surfaces began with the work of Lorenz in 1881. His publication of an analytical investigation of a constant temperature vertical plane wall was apparently the first of its kind. Lorenz made the assumption that the fluid temperature and velocity at a prescribed distance from the surface did not change with axial position. Disregarding this poor assumption, his results were comparable for moderate Prandtl number to results achieved later by more complicated analysis. Lorenz was the first investigator to show that the heat transfer rate varied as the $5/4$ power of the temperature difference between the surface and the ambient fluid. Also, he was the first to present heat transfer results that included all the pertinent variables associated with natural convection.

In 1930 Schmidt and Beckmann (1) applied the boundary layer approximations to the governing equations of continuity, motion, and energy for the case of a single isothermally heated flat plate in an effectively infinite pool of ambient fluid. Pohlhausen was able to perform a similarity transformation to reduce the set of partial differential equations to a pair of ordinary differential equations

for which a simultaneous series solution could be achieved. However, slow convergence of the solution necessitated that Schmidt and Beckmann provide two of the boundary conditions experimentally. The result for local Nusselt number, $Nu_x = 0.360 (Gr_x)^{0.25}$, was applicable, therefore, only to air ($Pr = 0.73$) for which the boundary conditions were obtained.

In 1939 Saunders (2) achieved an analytical solution for the heat transfer from a vertical flat plate with an isothermal wall. Experiments were also performed to substantiate the analytical results. An expression was given for average Nusselt number as $Nu_L = C(Gr_L Pr)^{0.25}$ where C is a function of Prandtl number. For the case of $Pr = 0.73$ the local Nusselt number would be $Nu_x = 0.344 (Gr_x)^{0.25}$ which is slightly less than Schmidt and Beckmann's exact result.

Saunders' results were obtained starting with two known boundary conditions and assuming a third order polynomial approximation for the temperature in the boundary layer. Solving the equations enabled a third boundary condition to be obtained. This numerical approximation was continued to a fifth order polynomial. The solution is of greater value than Schmidt and Beckmann's because it supposedly applies for a wide range of Prandtl numbers. For a Prandtl number of 0.023 the local Nusselt number is determined to be $Nu_x = 0.08 (Gr_x)^{0.25}$.

Saunders' experiments were performed in mercury and water. Two uniformly heated vertical flat plates were used. The plate heights were 2.80 and 4.65 cm. With a Prandtl number of 0.023, i. e., mercury, his experiments yielded $Nu_x = 0.09 (Gr_x)^{0.25}$ for the shorter plate and $Nu_x = 0.10 (Gr_x)^{0.25}$ for the longer plate. Saunders was the initial experimental investigator of natural convection heat transfer in a liquid metal.

To solve the governing equations of energy and momentum Eckert (3), in 1950, used an integral technique. He assumed equations for the velocity and temperature profiles in the boundary layer adjacent to an isothermal, plane, vertical surface. These approximations were introduced into the governing equations. The ensuing solution for the local Nusselt number yielded

$$Nu_x = 0.508 \left(\frac{Pr^2 Gr_x}{.952 + Pr} \right)^{0.25} .$$

This reduces to $Nu_x = 0.381 (Gr_x)^{0.25}$ for $Pr = 0.73$, indicating that this approximate approach yields results which compare favorably with Schmidt and Beckmann's (1) more detailed and nearly exact solution.

In 1953 Ostrach (4) studied the isothermal plane wall for Prandtl numbers of 0.01, 0.72, 0.733, 1, 2, 10, 100, and 1000. He detailed the simplification of the governing equations, pointing

out that a singular perturbation problem exists when considering large Grashof numbers. Using a basic assumption that the temperature difference between the heated surface and the ambient fluid was small and employing the boundary layer approximations Ostrach reduced the equations to two linear partial differential equations. This pair of equations was reduced to a pair of simultaneous ordinary differential equations by the introduction of similarity variables and subsequent rearrangement. Solution of these equations gave the average Nusselt number as

$$\text{Nu}_L = 4/3 \text{Nu}_{x/L} = \frac{4}{3} f(\text{Pr}) \text{Gr}_L^{0.25} .$$

Table T2.1 presents values of $4/3f(\text{Pr})$ vs. Pr . The values indicate the significant effect of Prandtl number upon the heat transfer.

Table T2.1. Heat transfer results of Ostrach (4).

$$\text{Nu}_L = 4/3 f(\text{Pr}) \text{Gr}_L^{0.25}$$

Pr	$4/3 f(\text{Pr})$
0.01	0.0765
0.72	0.475
1	0.535
2	0.675
10	1.10
100	2.06
1000	3.74

In 1955 Sparrow (5) solved the convection problem for both variable wall heat flux and variable wall temperature. Solutions were achieved by series expansion. The first term of the series results in an expression corresponding to uniform thermal conditions at the wall. The additional four terms account for the non-uniform thermal conditions. The solution is based upon the so-called Kármán-Pohlhausen method which involves writing the velocity and temperature distributions in the boundary layer as functions of y whose coefficients are functions of x . The wall heat flux or temperature distribution is expanded as a series in the parameter ϵ . Coefficients of identical powers of ϵ are brought together. It is necessary that each group of coefficients be equal to zero. The result is a pair of simultaneous differential equations for each power of ϵ . For the important case of uniform wall heat flux the result is

$$\text{Nu}_x = 0.62 \left(\frac{\text{Pr}^2 \text{Gr}_x^*}{0.8 + \text{Pr}} \right)^{0.20}$$

For the constant temperature wall the results are identical to those of Eckert (3), i. e.,

$$\text{Nu}_x = 0.508 \left(\frac{\text{Pr}^2 \text{Gr}_x}{0.952 + \text{Pr}} \right)^{0.25}$$

Solutions were achieved for Prandtl numbers of 0.01, 0.10, 0.70, 1.00, 10, 100, and 1000.

The authors later extended their work to include the low Prandtl numbers of 0.03 and 0.003 for the isothermal case (6). The result for local Nusselt number is $Nu_x = 0.565 (Gr_x Pr)^{0.25}$.

In 1956 Sparrow and Gregg (7) used a similarity transformation to solve the natural convection problem for the case of uniform wall heat flux. The Prandtl number range was 0.10 to 1000 and results were extrapolated to include $Pr = 0.01$. The results were presented graphically. Of interest is the result for a Prandtl number in the range of mercury; 0.023. In this case the local Nusselt number is $Nu_x = 0.161 (Gr_x^*)^{0.20}$. They also showed that the local Nusselt number for a uniform flux plate was greater than that for an isothermal plate by a constant factor that was independent of position and only slightly dependent on Prandtl number. Gebhart (8) made a similar comparison but reported results that appear to be slightly different.

Chang et al.(9), used a zeroth order perturbation solution to extend the results of Sparrow and Gregg (7) to include Prandtl numbers of 0.01 and 0.03 as well as to include the range from 0.10 to 1000. Solution was achieved for the uniform heat flux boundary condition. The zeroth order perturbation solution is identical to the similarity solution. Using potential flow theory the first order perturbation solution was also achieved. The results for this solution are somewhat more exact than the results for the similarity

solution due to the presence of an additional term in the series. A singularity at $x = 0$ in the zeroth order solution is magnified with increasing order of perturbation so that additional terms in the series caused difficulties in achieving a solution, especially near the leading edge of the plate. Chang's first order perturbation solution is given by $Nu_x = 0.632 Pr^{0.37} (Gr_x^*)^{0.20}$. For the case of $Pr = 0.023$ the result is $Nu_x = 0.157 (Gr_x^*)^{0.20}$.

Kuiken (10) used a singular perturbation technique to solve the boundary layer equations for the isothermal vertical plate and the case of low Prandtl numbers. The method employed is that of matched asymptotic expansions. The purpose of the work was to solve the equations and present the results explicitly in terms of Prandtl number while maintaining the accuracy of an exact solution. The heat transfer results are given by

$$Nu_x = (0.60 - 0.324 Pr^{1/2}) (Gr_x Pr^2)^{1/4}$$

In recent years the interest in experimental investigations for liquid metals has intensified. Nearly thirty years after Saunders completed the initial heat transfer investigations for a liquid metal Julian (11) measured the heat transfer from a uniform flux plate immersed in a pool of mercury. With a value for Prandtl number of 0.022 he correlated his data by $Nu_x = 0.196 (Gr_x^*)^{0.188}$.

A relatively thorough background has been presented here with regard to the vertical flat plate. It will be of great interest in comparing results to those achieved for the vertical cylinder. To get additional background involving natural convection heat transfer for other situations and geometries, Gebhart (8), Chang et al. (9), and White (12) present excellent reviews on the subject.

Of greater interest to the current research is work involved with vertical cylinders. There has been significantly less work done with this geometry than has been done with the flat plate. A review of what has been accomplished follows.

2.2 Circular Cylinders

Experimental investigations of natural convection heat transfer from vertical cylinders have been performed for cylinders with diameters on the order of a thousandth of an inch (13, 14) up to several inches. A notable conclusion concerning very small diameter wires was presented by Elenbaas (15) who stated that the influence of the wire diameter upon the heat transfer was extremely small.

The earliest available study on large diameter vertical cylinders was presented by Griffiths and Davis (16) in 1922. They examined the laminar natural convection heat transfer from a constant temperature cylinder to air. McAdams (17) reported the results for the

average heat transfer coefficient as $h_c = 0.4 \left(\frac{\Delta T}{D}\right)^{1/4}$. For cylinder heights less than 1.5 feet a correction factor is available.

Carne (18), in 1937, performed experiments similar to those of Griffiths and Davis. The heat transfer results were tabulated.

In 1942 Elenbaas (19) derived an analytical expression for the heat transfer from a vertical cylinder of diameter d , with conditions based on w , the wall temperature, and m , the mean temperature defined as $T_\infty + \frac{T_w - T_\infty}{2}$. His expression is

$$\text{Nu}_{d,w} \exp\left(-\frac{2}{\text{Nu}_{d,m}}\right) = 0.6 \left[(\text{Gr}_{d,w} \text{Pr}_w) \cdot \frac{d}{h} \right]^{1/4},$$

which reduces to $\text{Nu}_{h,w} = 0.6 (\text{Gr Pr})_{h,w}^{1/4}$ for the flat plate, i.e., as $d \rightarrow \infty$. The subscript h represents the plate height. In an attempt to verify his analysis for cylinders Elenbaas set up experiments in air similar to those of Griffiths and Davis (16), and Carne (18). The results showed discrepancies of as much as 15%.

In 1948, Touloukian et al. (20), used water and ethylene glycol as the heat transfer medium to study natural convection from a constant temperature vertical cylinder. They chose to work with this geometry to study the natural convection phenomenon because of its advantages over the flat plate. Most important were the horizontal symmetry and elimination of edge effects. The results were given by $\text{Nu}_x = 0.544 (\text{Gr Pr})^{0.25}$. Notice that there is no

explicit dependence on diameter.

Sparrow and Gregg (21) transformed the equations of the cylindrical boundary layer using a series expansion of the dependent variables. Sets of simultaneous ordinary differential equations were obtained. The first three sets of equations were solved for the case of constant surface temperature using numerical integration. The Nusselt number was given as a sum of the three solutions. It was found that the analytical results for a constant temperature flat plate was a common factor in each term of the Nusselt number correlation. Therefore, a ratio of the cylinder Nusselt number to the flat plate Nusselt number could be easily obtained. Solutions were acquired for Prandtl numbers of 0.72 and 1.00. The results showed that the Nusselt number for a cylinder was greater than that for a flat plate and that the deviation was more extreme for lower Prandtl numbers. It was determined that for the heat transfer results of the cylinder to be within five percent of the flat plate results it was necessary that

$$\frac{D}{L} \geq \frac{35}{Gr_L^{1/4}}$$

Thus, the effect of curvature could be directly inferred.

Millsaps and Pohlhausen (22, 23) showed that, if the temperature difference between the surface and the fluid increased linearly

from zero at the leading edge, a similarity transformation of the governing equations could be accomplished. Solutions of the equations were obtained for Prandtl numbers of 0.733, 1, 10, and 100. Gebhart (8) found that the results could be well approximated by the equation

$$\frac{hD}{k} = 1.058 (Gr')^{1/4} \left(\frac{Pr^2}{4 + 7 Pr} \right)^{1/4},$$

where

$$Gr' = \frac{\beta g D^4}{\nu} \left(\frac{dT}{dx} \right)_o$$

Nagendra et al. (24), investigated free convection heat transfer from wires and cylinders in an attempt to support their analytical results. The cylinder used in their study was 0.315 inches O.D. and twelve inches long. The heat transfer medium was water. The surface approximated the isothermal case. The results are classified according to the range of $Ra_D \frac{D}{L}$. The experimental results were within ten percent of values predicted by the following equations:

Cylinder classification	$Ra \cdot \frac{D}{L}$ range	$Nu_D =$
short (i. e., flat plates)	$10^4 < Ra \cdot \frac{D}{L}$	$0.57 (Ra_D \frac{D}{L})^{0.25}$
long	$.05 < Ra \cdot \frac{D}{L} < 10^4$	$1.30 (Ra_D \frac{D}{L})^{0.16}$
wires	$Ra \cdot \frac{D}{L} < .05$	$0.87 (Ra_D \frac{D}{L})^{0.05}$

In 1970, a year after the above results were published, the same authors (25) presented results for the boundary condition of uniform heat flux from a circular cylinder. This was the only paper to be found that handled this boundary condition completely. The analysis involved a similarity transformation of the governing equations. A numerical iteration technique developed by the authors achieved the following results for the same cylinder classification scheme as given above:

Cylinder classification	$Nu_D =$
short	$0.55 (Ra_D^* \frac{D}{L})^{0.20}$
long	$1.33 (Ra_D^* \frac{D}{L})^{0.14}$
wires	$0.90 (Ra_D^* \frac{D}{L})^{0.048}$

To determine the category into which a cylinder belongs it is necessary to replace $q \frac{D}{k}$ in the modified Rayleigh number by $\overline{T_w - T_\infty}$. The authors point out that the results for short cylinders are within eight percent of the flat plate results and for this reason they consider a short cylinder to be essentially a flat plate.

III. EXPERIMENTAL DESIGN

3.1. Apparatus

3.1.1 Construction of the Heated Cylinders

The basic component of the vertical cylinders are the heaters, purchased from Electrofilm, Inc., of North Hollywood, California. The heater design consists of a chemically etched, printed circuit type element, permanently vulcanized between layers of silicone rubber reinforced with fiberglass. The lead wires emerge from a one-half inch by one inch tab that extends from the top of the heater. Nominal heater thickness is 0.045 inches while the tab thickness is 0.090 inches.

Three cylinders were constructed and tested. The outside diameters were 0.590, 1.355, and 2.108 inches. (In subsequent discussion of the heaters, these will be referred to as cylinder 1, cylinder 2, and cylinder 3, respectively.) The tolerance on the diameter was measured to be ± 0.005 inches. Each heated section was 3.85 inches high. The three completed cylinders are shown in Figure F3.1.

The heaters were form fit to the proper diameter core to assist in obtaining a uniform surface. In order to remove the heaters from the cylindrical mold after manufacturing, allowance was made

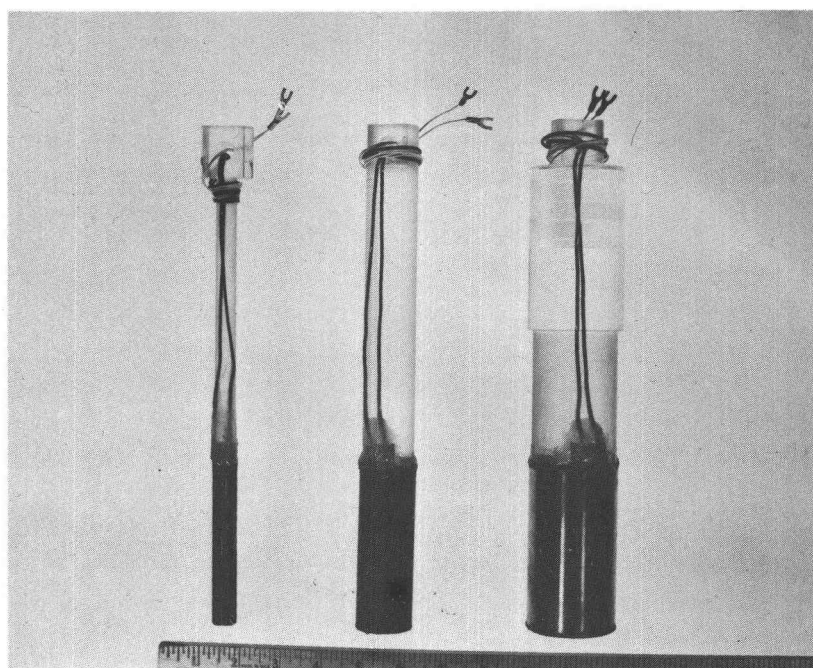


Figure F3.1. The three completed cylinders.

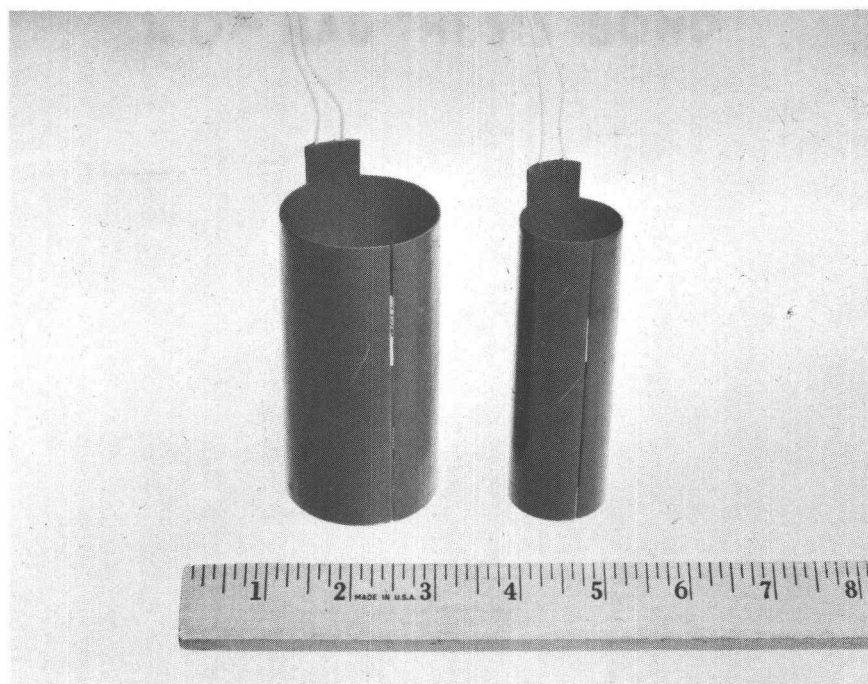


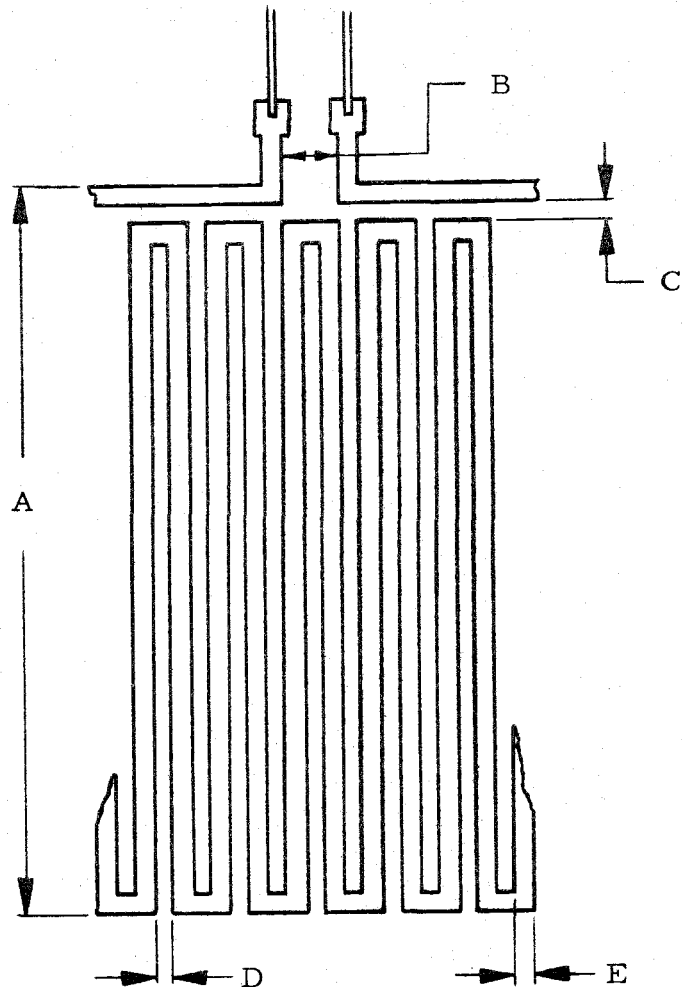
Figure F3.2. Heaters before assembly.

for an axial seam along the side of each heater opposing the tab. The features of the heaters are shown in Figure F3.2. A sketch of the circuit and the dimensions of the elements are presented in Figure F3.3.

Construction of the heated cylinders involved attaching the heaters to a machined acrylic core. When the heaters were placed in their required position on the core a two-sided mylar tape was wrapped tightly around the outer surface. The resulting friction between the core and heater assisted in securing the heater in the correct position.

Each heater and core assembly was inserted into a pre-formed mild steel sleeve having a wall thickness of 0.010 inches. The sleeve adhered to the outer tape surface. This smooth sleeve served as the outer surface of the cylinder assembly. To prevent infusion of mercury into the heater, silicone rubber sealer was applied along all exposed edges.

The mild steel sleeve, made from 0.010" cold rolled shim stock, was pre-formed to approximately the desired diameter by rolling. A male-female cylindrical die assembly of correct diameter was machined with an allowance for the sleeve to be inserted between the two parts. After insertion into the die the sleeve was stress-relieved by heat treatment; when cooled it retained the exact cylindrical shape desired.



	Cylinder 1	Cylinder 2	Cylinder 3
A	3.80	3.80	3.80
B	0.270	0.245	0.238
C	0.040	0.040	0.040
D	0.023	0.026	0.027
E	0.026	0.077	0.129

Tolerances: E: ± 0.002 ; Others: ± 0.010 ;
 Dimensions are in inches.

Figure F3.3. Circuit pattern of heaters with dimensions.

Before the construction of the cylinders the heaters were x-rayed to determine as closely as possible the location of the resistance elements. All material considered to be non-heating were trimmed away. Care was taken to machine the acrylic core to a diameter such that the vertical seam on the back side of the heater would close when the heater was placed over the core. The outer metal sleeve was then sized to fit precisely over the heated area.

The vertical cylinders were supported in the mercury by a brace extending across the top of the mercury tank. The cylinder core, made entirely from acrylic rod, extended down into the mercury about ten inches. The leading edge of the core coincided with the leading edge of the heater. This placed the heated section approximately in the middle of the mercury pool. Because the heater was suspended in the mercury in this way, an unheated trailing section was present and had a diameter essentially equal to that of the heated section.

3.1.2 Basic Test Section

The basic component of the experimental system is shown in the schematic of Figure F3.4 and in Figure F3.5. The heated vertical cylinder [1]¹ is shown suspended in the mercury pool [2] from the

¹Numbers in brackets refer to respective items in Figure F3.5.

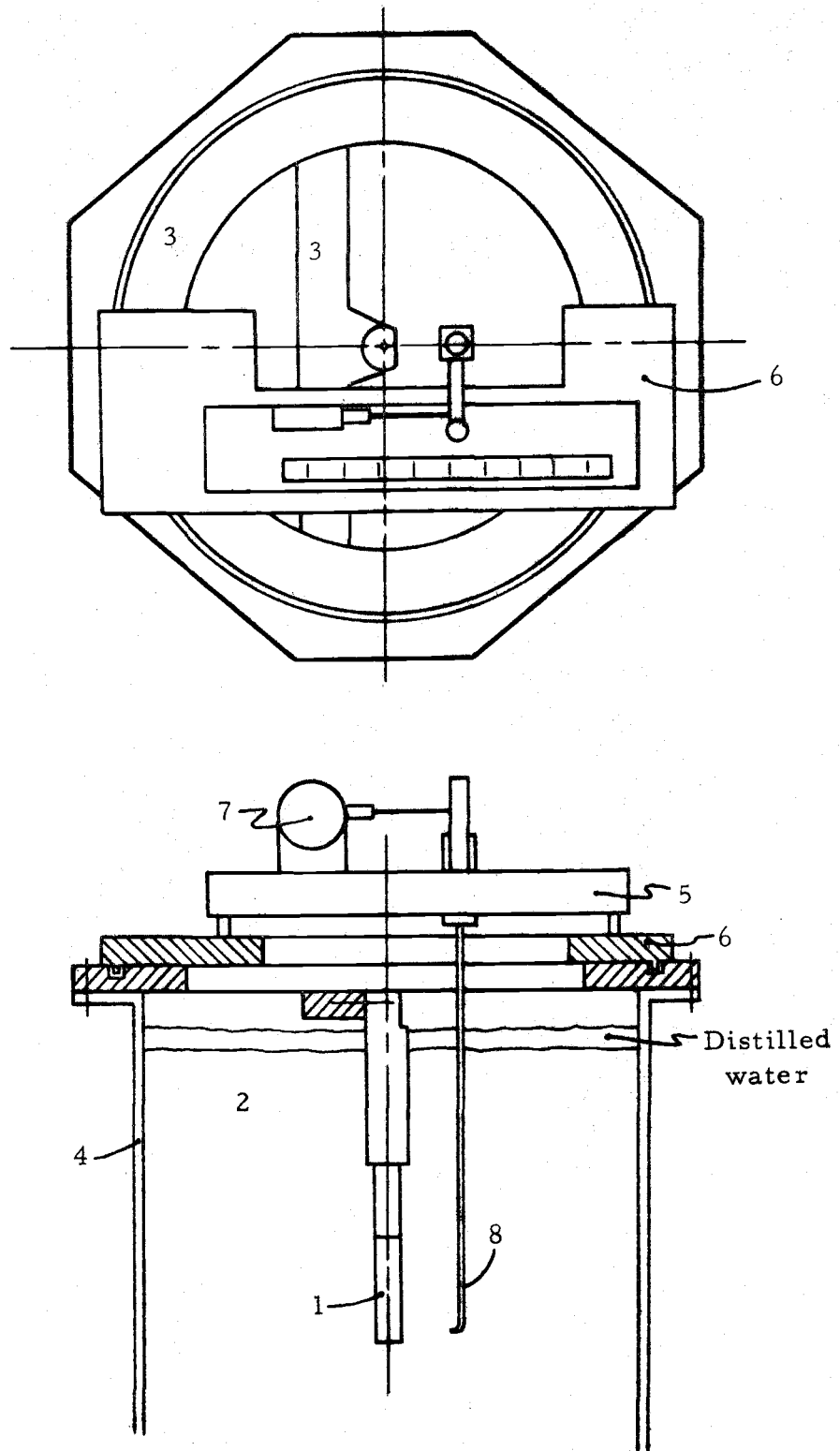


Figure F3.4. Schematic of basic test section.

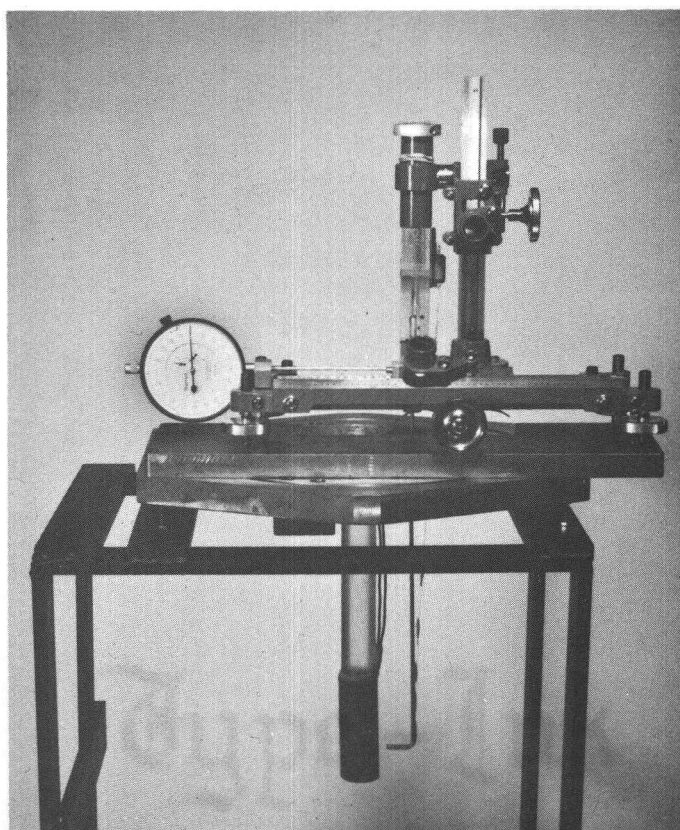


Figure F3.5. Basic test section.

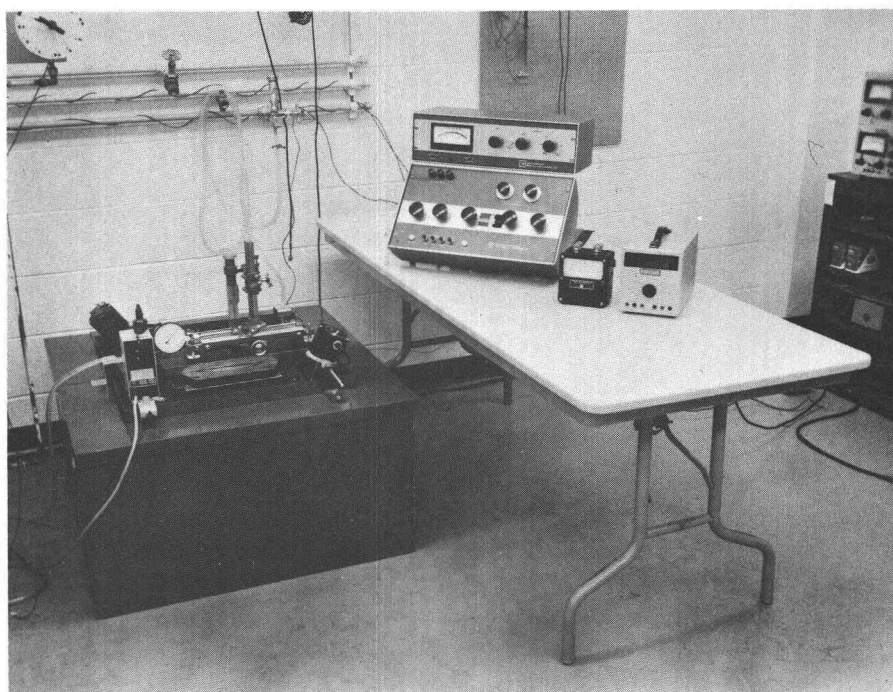


Figure F3.6. Overall view of apparatus.

brace [3] that is mounted to the mercury tank [4]. A traversing mechanism [5] is mounted to a horizontal table [6] which can rotate relative to the brace. A Starrett dial indicator [7], mounted to the traverse mechanism, assisted in precise location of radial position of the probe. The center of rotation of the table coincides with the center axis of the fixed vertical cylinder. A sheathed iron-constantan thermocouple manufactured by Omega Engineering, Inc., of Stamford, Connecticut, is attached to a probe shaft [8] which is suspended from the traverse mechanism. The thermocouple was calibrated with a quartz thermometer. The system allows the thermocouple to be rotated through 180° about the surface of the cylinder. Within this circumferential range surface temperatures and radial temperature profiles can be measured for any axial position.

3.1.3 Additional Equipment

An overall view of the experimental system is shown in Figure F3.6.

Ambient temperature in the mercury was maintained constant by surrounding the mercury tank with a well stirred, temperature controlled water bath. To remove heat from the water bath, copper tubes were immersed in the water and cold water was allowed to circulate through these tubes. To maintain the isothermal condition a temperature sensitive heater was suspended into the water to create

a balance with the heat added from the mercury and the heat removed via the cooling tubes. The water bath is further insulated with Zonolite vermiculite packed loosely within a rectangular box surrounding the water tank.

Electrical input was supplied by a D. C. power supply, specifically a Magnet Supply by Manson Laboratories, Inc., Model M25-702. The power determination was made from the current-voltage product. Current was measured by means of a Weston Instrument, Inc., ammeter. Voltage was obtained using a Honeywell multicomponent digital meter, model 333 R.

Thermocouple electrical output was measured using a Leeds and Northrup K-4 Potentiometer in conjunction with a Leeds and Northrup D. C. Null Detector, model 9828. Additional related equipment included a standard cell from the Eppley Laboratory, Inc., and a constant voltage supply, 2 volts D. C., by Leeds and Northrup.

3.2 Procedure

Heat transfer results were desired in the form of local Nusselt number, calculated according to the equation

$$Nu_x = \frac{qx}{k\Delta T}$$

The surface heat flux, q , was determined by dividing the product of the current and the voltage by the known surface area of the heated section. The conductivity was assumed to be known exactly. An

equation for k was taken from a paper by Powell and Tye (26). All other properties, such as those present in the Grashof number, are evaluated from information given in the Liquid Metals Handbook (27).

The traverse mechanism enabled the precise location of the thermocouple probe to be known. The vernier on the mechanism allowed the probe location to be adjusted to ± 0.0005 inches in either the axial or radial direction. The vernier reading when the probe was at the leading edge of the cylinder was determined prior to insertion of the apparatus into the mercury. Using this reading, prescribed values of x could be readily marked off.

The final term in the Nusselt number, ΔT , required the separate determination of ambient and surface temperature. The traverse mechanism had enough travel such that the thermocouple probe could be located at least two inches radially outward from the heated surface and two inches below the leading edge of the cylinder. Ambient temperature measurements were taken at this position. It was assumed that the mercury tank was large enough (12" x 12" x 16") that it could be considered an essentially infinite medium. This was proved by observing temperatures at two inches from the surface for the range of axial positions. Ambient temperature stratification did not occur. The surface temperature was taken as the indicated temperature when the probe tip was in contact with the surface.

Locating the probe at the surface was not a critical procedure

unless temperature profiles were sought. Obtaining a profile required taking a temperature reading at the surface and at radial positions of 0.01, 0.02, 0.03, 0.04, 0.05, 0.06, 0.08, 0.10, 0.15, and 0.30 inches from the surface. A Starrett dial indicator, readable to ± 0.00005 " was mounted to the traverse mechanism to assist in accurately placing these radial increments. However, to prevent all the points from being misaligned, the surface had to be located correctly. The probe was advanced toward the surface in small increments and the change in temperature was observed. As the probe neared the surface the temperature rise would become quite pronounced. When the probe contacted the surface the temperature would no longer rise, but, due to the flexibility of the probe shaft, further travel was possible and usually occurred. To attempt to get the probe in contact with the surface without deflecting the shaft, the probe was backed away from the surface until the temperature was observed to drop. The critical adjustment was completed by observing temperature changes for very small inward and outward increments of probe travel. If ideal surface contact was achieved then the first radial increment of 0.01 inches would, indeed, place the probe tip a distance of 0.01 inches from the surface.

The reference junction for the thermocouple was positioned about one inch from the bottom of a small tube filled with mercury. This tube was then immersed in a bath of ice and distilled water.

3.3 Sources of Error

The heat transfer results of this report are given by the relation

$$\text{Nu}_x = C(\text{Gr}_x^*)^n$$

or

$$\frac{qx}{k\Delta T} = C \left(\frac{\beta g}{2 \nu k} q x^4 \right)^n$$

The properties are assumed to be known exactly and, therefore, for any given measurement, the variables of concern become

$$\frac{qx}{\Delta T} = C' (qx^4)^n$$

or

$$C' = \frac{x^{1-4n} q^{1-n}}{\Delta T}$$

The accuracy of the heat transfer results is seen to be a function of only three terms, these being x , q , and ΔT . From the experimental results, n is found to vary with diameter. In terms of this analysis, however, it should suffice to let n equal 0.2. Then

$$C' = \frac{x^{0.2} q^{0.8}}{\Delta T}$$

Factors that could degrade the accuracy of these terms come

from three different categories. One would involve systematic errors which would expose themselves in the same effect for all measurements. Another would be random errors involved with the accuracy to which a reading can be consistently taken. A third would be the predictable error involved with the uncertainty of the instrument readings.

It is reasonable to neglect the last two sources of error. Axial position is measured on the order of inches while the locating instrument is readable to a thousandth of an inch. The temperature difference in millivolts is on the order of tenths of a millivolt while the potentiometer can be read to a value of a ten-thousandth of a millivolt. The power input is a product of a voltage and current measurement. The voltage is on the order of hundreds while the voltmeter is readable to a tenth. Current is possibly the least accurate measurement involved, with absolute values on the order of unity and a readability of about two hundredths. On the basis of these numbers, the predictable error involved with the evaluation of C' is approximately two percent, certainly a tolerable figure.

The final regression equation for each cylinder was evaluated from the combination of two independent sets of data, i. e., data that had been taken on two different days. Each individual group of data was regressed in order to obtain a quantitative estimate of the repeatability of the results. These regressions may be referred to

in the results section as equations E4. 2a through E4. 2f. The pairs of regression equations for each cylinder were compared for various Grashof numbers. The results of the comparison are given in Table T3. 1. The regression equations are included here to substantiate the comparison.

Table T3. 1. Nu_x vs. Gr_x^* as calculated from regression equations E4. 2.

Cyl.	Equation E4. 2	Regression equation for Nu_x	Values of Nu_x for Gr_x^* of:	
			10^6	10^{10}
1	a.	$0.221 Gr_x^{*0.193}$	3.198	12.169
	b.	$0.202 Gr_x^{*0.198}$	3.119	12.261
2	c.	$0.239 Gr_x^{*0.184}$	3.050	10.896
	d.	$0.190 Gr_x^{*0.195}$	2.814	10.828
3	e.	$0.221 Gr_x^{*0.186}$	2.887	10.426
	f.	$0.233 Gr_x^{*0.185}$	2.979	10.655

Most variation is obviously going to occur in the results of cylinder 2, for it can be readily observed that the two regressions associated with this cylinder have the greatest variation in slopes and intercepts. The maximum variation is about eight percent at a Grashof number of 10^6 . Of course the variation increases with

decreasing Grashof number but the range of Grashof number from 10^6 to 10^{10} is of primary concern. The variations for the other two cylinders are seen to be much less.

Assuming that random errors are in part responsible for the variations of the results it seems justified to neglect such errors since they seem to be quite small. That is, if the results are substantially incorrect it is unlikely to be due to randomness. A further indication that random reading errors are small is the value of the correlation coefficient, R^2 . For each of the final regression equations the value of R^2 is greater than 0.995. The correlation coefficient, R^2 , is a ratio of the sum of the squares of two terms. The sum of the squares of the difference between the experimental value and the mean is divided by the sum of the squares of the difference between the value predicted by the regression and the mean. The mean is the mean value of the dependent variable for all the data. A value of R^2 of 1.00 would indicate that all the experimental points fit exactly on the regression curve.

Random reading errors are probably most prevalent in the measurement of ΔT . The measurement of the ambient temperature and the surface temperature was not instantaneous. The ambient temperature was measured first, followed immediately by a measurement of a surface temperature. Slight drifts in the ambient temperature during the surface locating procedure would certainly affect ΔT .

It was not until the experimental work was nearly completed that the procedure was altered to use the ambient fluid as the reference junction, thereby instantaneously measuring ΔT .

The third potential source of error in the results is that due to systematic discrepancies in the experimental technique or in the apparatus. When considering the validity of the results, the possibility of such errors is of the greatest interest. Consider individually the three terms involved in the determination of C' , i. e., x , q and ΔT .

The axial position is measured as the distance from the leading edge of the heater. To establish this point required a judgment of the location of the leading heater resistance element with respect to the leading edge of the cylinder. Care was taken to construct the cylinders so that the leading edge of the outer sleeve would correspond physically to the leading edge of the heated section, but the potential for this systematic type of error exists. An estimate of its possible extent would be ± 0.03 inches. At an x position of 0.40 inches this could produce an error of 7.5%.

The power input as determined by the current and voltage product should be reasonably precise as the ammeter and voltmeter were calibrated by comparison to similar meters. The heat flux, q , however, could be systematically in error due to evaluation of the heated area. Again, care was taken to trim away any unheated

material but this does not negate the possibility for error in the exact evaluation of area. An estimated value of this error is $\pm 3\%$ for the heat flux.

Another potential problem existed in the ability to know the heat flux accurately. This involved the possibility that heat could have been conducted axially within the acrylic core.

The hottest region in the core was beneath the heater at the trailing edge of the heated section. This created a potential for heat transfer by conduction in either direction. If the heat was transferred down the core the result would have been a deviation from the constant heat flux case towards the constant temperature boundary condition. If heat transfer had occurred via axial conduction in the positive x direction the true heat flux measurement would also have been altered. The outcome of such errors would be to increase the Nusselt number.

To check that the losses incurred through axial conduction were, indeed, negligible, a simple analysis can be performed. Assume a uniform temperature over the trailing edge cross-section. Use the leading edge of the cylinder as a zero reference. The downward axial heat rate would be approximately $q = k \frac{\Delta T}{L}$ where ΔT is the difference between the average temperature over the trailing edge cross-section and the zero reference, and L is the length over which the temperature difference occurs. The trailing edge cross-sectional

temperature might be on the order of 60°F above the leading edge for a surface heat flux of 2500 Btu/hr ft^2 (440 Btu/hr for cylinder 3). This relatively high temperature is due to the thermal resistance between the heater elements and the mercury. In this case, L is approximately one-third foot. Therefore, the axial heat rate would be on the order of 15 Btu/hr ft^2 ($1/3 \text{ Btu/hr}$ for cylinder 3). This is certainly a negligible quantity compared to the total surface heat flux.

Heat may also be conducted in the upward direction. The heated mercury flowed along the surface of the cylinder beyond the trailing edge of the heater. Assuming that the core temperature approaches the temperature of the adjacent mercury at a distance, L , of two inches above the trailing edge then the positive axial conduction would be about 30 Btu/hr ft^2 ($2/3 \text{ Btu/hr}$ for cylinder 3), again a negligible amount relative to the surface flux.

The third term involved with the evaluation of C' is ΔT . The only apparent source for error exists with the measured value of surface temperature. Such error is experienced because when the thermocouple probe is in contact with the surface the thermocouple junction, being buried in a bead of stainless steel, remains approximately 0.003 inches from the surface. The conductance from the mercury to the stainless steel probe wire is high and therefore it is logical to assume that the fluid temperature at 0.003 inches from the surface manifests itself upon the thermocouple junction at that point.

To evaluate the error, consider a particular situation which represents a probable worst case; $x = 0.40''$, $q = 1250 \text{ Btu/hr ft}^2$, $\Delta T = 0.0868 \text{ M. V.}$ and $(\frac{dT}{dr})_o = 0.643 \text{ M. V. /in.}$ The true surface temperature should be increased by an additional $(0.003 \text{ in}) \times (0.643 \frac{\text{M. V.}}{\text{in}}) = 0.0019 \text{ M. V.}$ The error is $\frac{0.0019}{0.0868} = 2.2\%$.

To summarize the total effect of the major sources of systematic error, the square root of the sum of the squares of the individual errors is evaluated. Each squared term is multiplied by its respective exponent prior to summation. In this way, the combination of errors in C' are 4.8%, calculated as follows:

$$\begin{aligned} \text{Error} &= \left(\sum_{i=1}^j n_i (E_i)^2 \right)^{1/2} \\ &= \left(.2 (E_x)^2 + .8 (E_q)^2 + (E_{\Delta T})^2 \right)^{1/2} \\ &= \left(.2 (7.5)^2 + .8 (3)^2 + (2.2)^2 \right)^{1/2} \end{aligned}$$

IV. HEAT TRANSFER RESULTS

Prior to any experimental investigation it was anticipated that the effect of a finite curvature upon the natural convection heat transfer from a vertical surface would be manifested in a cylinder Nusselt number that would be larger than that for a flat plate. The heat transfer results show this to be correct. For the three cylinders that were employed in the investigation, local Nusselt numbers increased with increased curvature (i. e., decreased diameter) for a given Grashof number. The trend was apparent over the entire range of Grashof number which was 10^5 to 10^{10} . It is of significant interest to note that at Grashof numbers as high as 2×10^{10} there was no pronounced evidence of the onset of transition from laminar to turbulent flow. For the flat plate, transition Grashof numbers are reported to be on the order of 5×10^9 (28).

For each cylinder approximately two hundred data points were obtained. This is certainly enough to be assured that no discrepancies exist in the results due to an inadequate sampling of data. The regression equations for the data were obtained by computer analysis.

The heat transfer correlations are as follows:

$$\begin{aligned}
 \text{a. Cyl. 1 : } Nu_x &= 0.216 (Gr_x^*)^{0.195} \\
 \text{b. Cyl. 2 : } Nu_x &= 0.217 (Gr_x^*)^{0.189} \\
 \text{c. Cyl. 3 : } Nu_x &= 0.224 (Gr_x^*)^{0.186}
 \end{aligned}
 \tag{E4.1}$$

The correlation coefficient, R^2 , for the three regressions were 0.997, 0.995, and 0.998, respectively. Plots of the data are given in Figures F4.1, F4.2, and F4.3. The data points R, F, and L refer to the right, front, and left circumferential positions about the cylinder surface. It is apparent from the random appearance of the three marks that heating was axisymmetric.

Data were taken for each cylinder on two different days and the two groups of data were combined in order to obtain the regression equations given above. Each individual group of data was regressed in order to observe any changes. The results of these regressions are as follows:

$$\begin{array}{ll}
 \text{a.} & \text{Nu}_x = 0.221 (\text{Gr}_x^*)^{0.193} \\
 \text{Cyl. 1} & \\
 \text{b.} & \text{Nu}_x = 0.208 (\text{Gr}_x^*)^{0.198} \\
 & \\
 \text{c.} & \text{Nu}_x = 0.239 (\text{Gr}_x^*)^{0.184} \\
 \text{Cyl. 2} & \hspace{15em} (\text{E4. 2}) \\
 \text{d.} & \text{Nu}_x = 0.190 (\text{Gr}_x^*)^{0.195} \\
 & \\
 \text{e.} & \text{Nu}_x = 0.221 (\text{Gr}_x^*)^{0.186} \\
 \text{Cyl. 3} & \\
 \text{f.} & \text{Nu}_x = 0.233 (\text{Gr}_x^*)^{0.185}
 \end{array}$$

By a simple trial and error procedure it was found that the data could be made to fit one generalized equation, specifically

$$\text{Nu}_x = 0.226 \left(\frac{D}{L}\right)^{0.032} (\text{Gr}_x^*)^{0.183} \left(\frac{D}{L}\right)^{-0.032} \quad (\text{E4. 3})$$

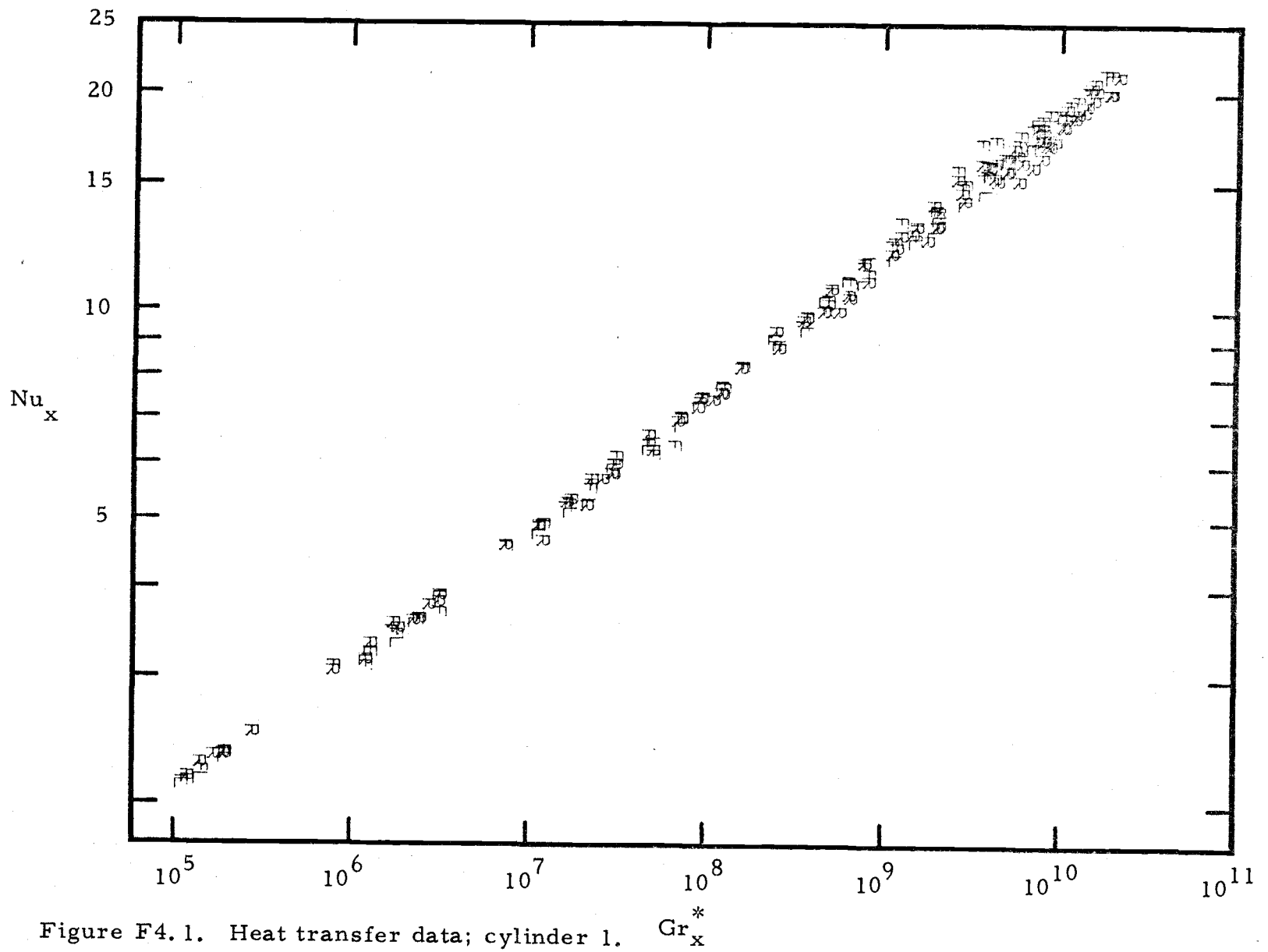


Figure F4.1. Heat transfer data; cylinder 1.

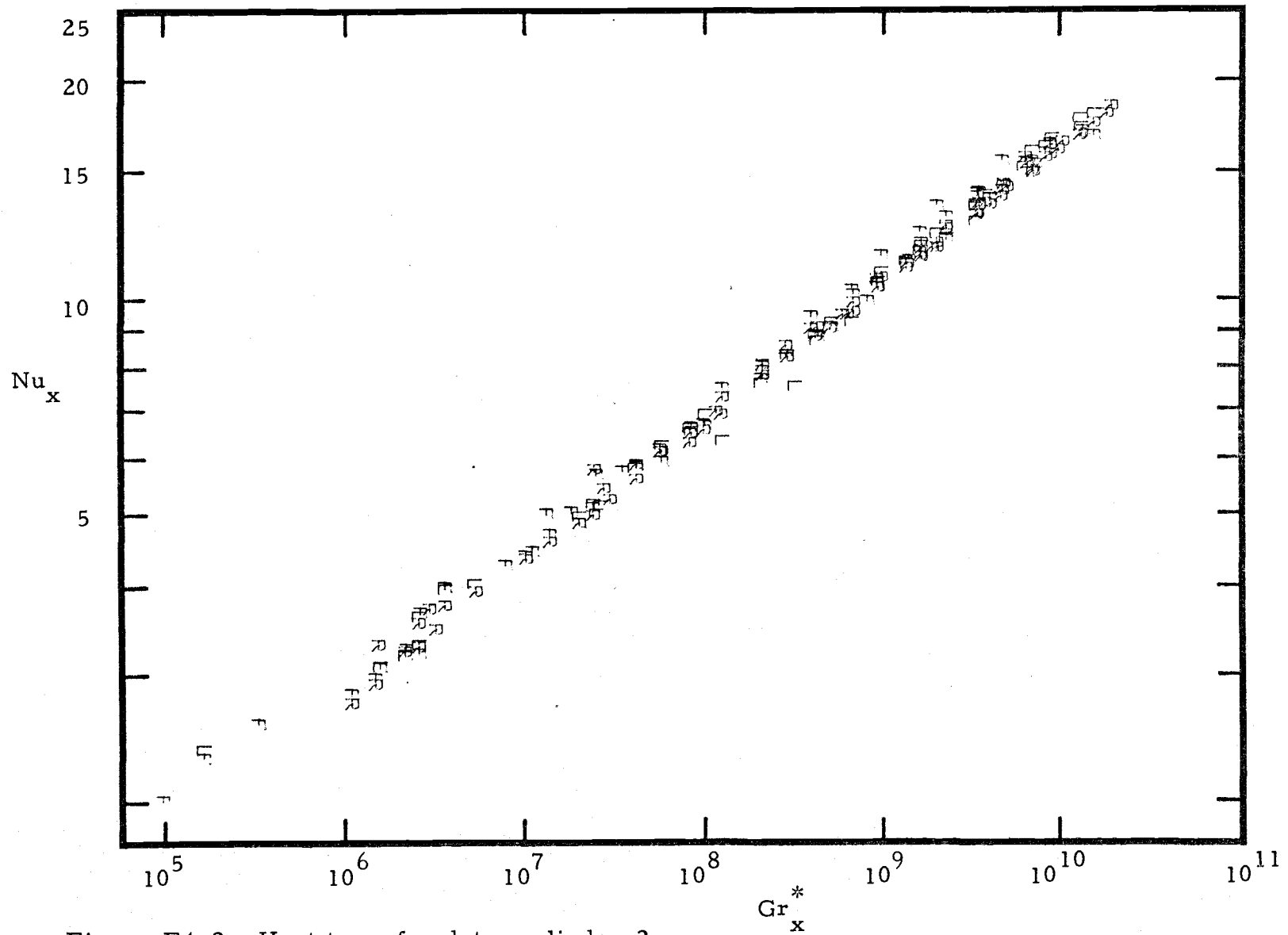


Figure F4.2. Heat transfer data; cylinder 2.

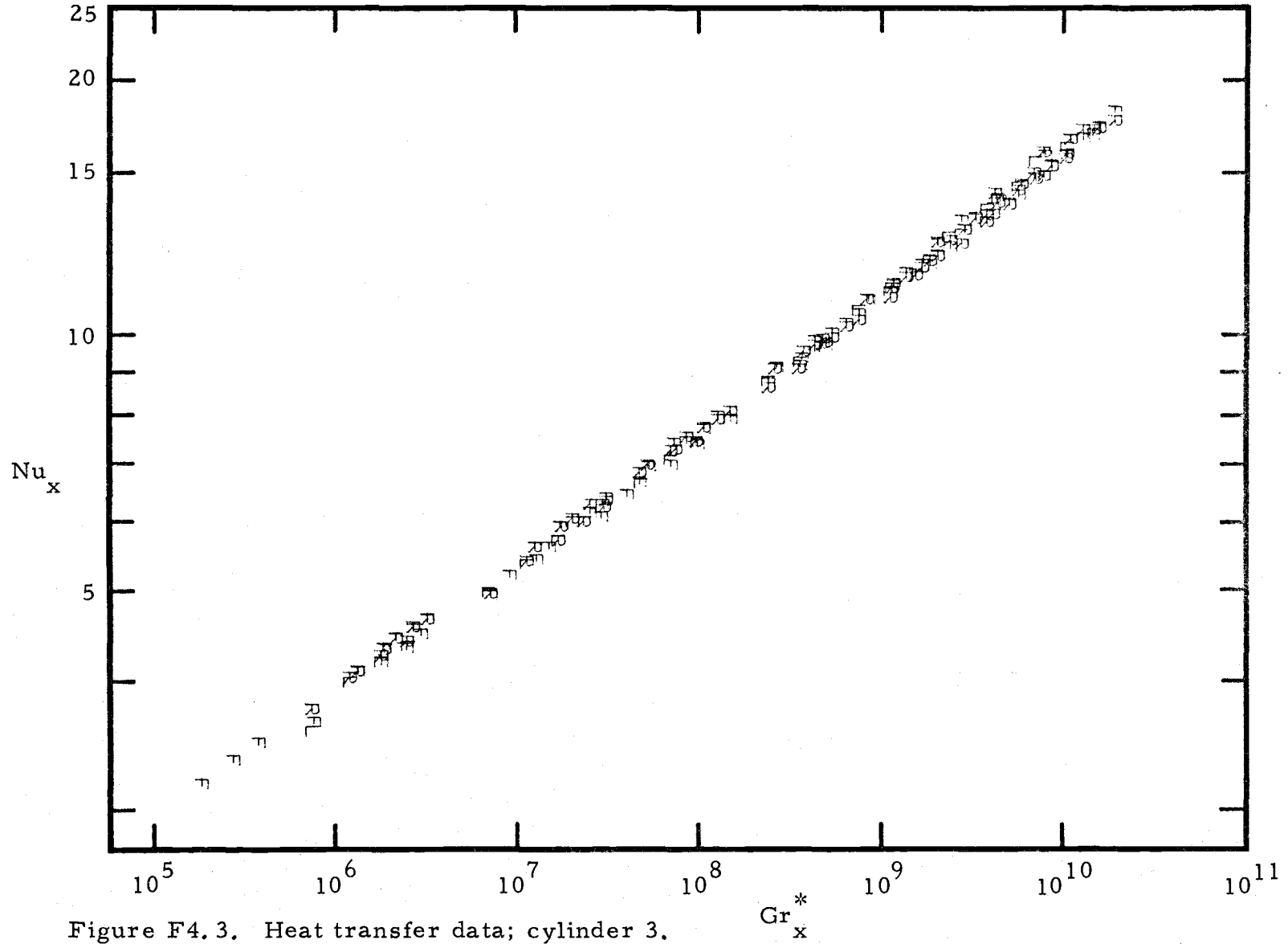


Figure F4.3. Heat transfer data; cylinder 3.

This equation predicts the results of the individual regressions to within $\pm 2\%$. The utility of this equation is that it can be applied with some confidence over a range of $\frac{D}{L}$ from 0.15 to 0.55. Extrapolation of equation E4.3 beyond these limits is not advised, however.

Preceding a closer examination of the generalized equation, one might conclude from the very small powers on the $\frac{D}{L}$ terms that effects of curvature are all but negligible over the range of observed data. For some purposes this may be true. Therefore, it may be acceptable to use a simpler expression for local Nusselt number which was achieved by combining the 592 total data points for the three cylinders and regressing the entire group. The result of the regression was

$$\text{Nu}_x = 0.216 (\text{Gr}_x^*)^{0.191} \quad (\text{E4.4})$$

In the worst case, at $\text{Gr}_x^* = 10^{10}$, deviations from the individual regressions are $+9.2\%$ and -7.5% . The plot of the combined data is shown in Figure F4.4. The numerals 1, 2, and 3 represent the contributions from cylinders 1, 2, and 3, respectively.

Extrapolation of the data to determine the limit at large diameter, i. e., flat plates, may not be valid but will at least provide a basis for comparison of the results for a cylinder to those of a flat plate. The extrapolation was accomplished by plotting local Nusselt numbers vs. $\frac{L}{D}$ at a given Grashof number. A smooth curve was

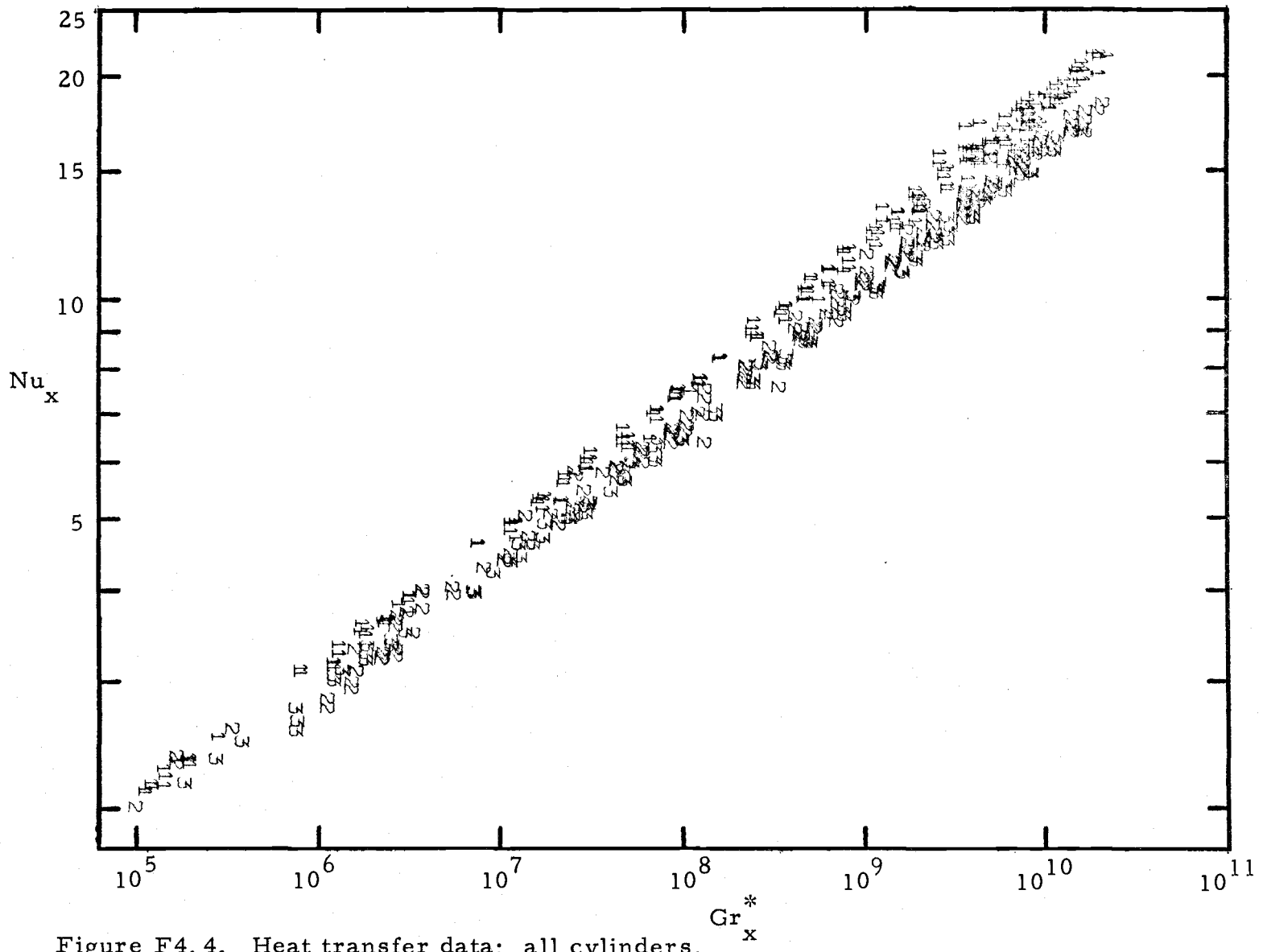


Figure F4.4. Heat transfer data: all cylinders.

made to fit through the three available points and was continued to the intercept. This was done for four Grashof numbers. The intercepts were determined for each and these values of Nu_x at $\frac{L}{D} = 0$ were plotted against Grashof number.

The graphical extrapolations are shown in Figure F4.5. The data for the intercepts is presented in Table T4.1. These points are plotted in Figure F4.6. Since the intercept values obtained via extrapolation are questionable, it is sufficient to determine graphically the equation for the resultant line. The result is

$$Nu_x = 0.232 (Gr_x^*)^{0.181} \quad (E4.5)$$

Table T4.1. Values of Nu_x at $\frac{L}{D} = 0$ for values of Gr_x^* .

Gr_x^*	Nu_x
10^6	2.84
10^7	4.32
10^8	6.58
10^9	9.92

The regressions for the cylinders show that for decreasing curvature the exponent of Gr_x^* decreases while the coefficient increases. As can be observed, equation E4.5 has the smallest exponent and largest coefficient of either of the cylinder regressions. The fact that this equation fits the trend is not surprising, however,

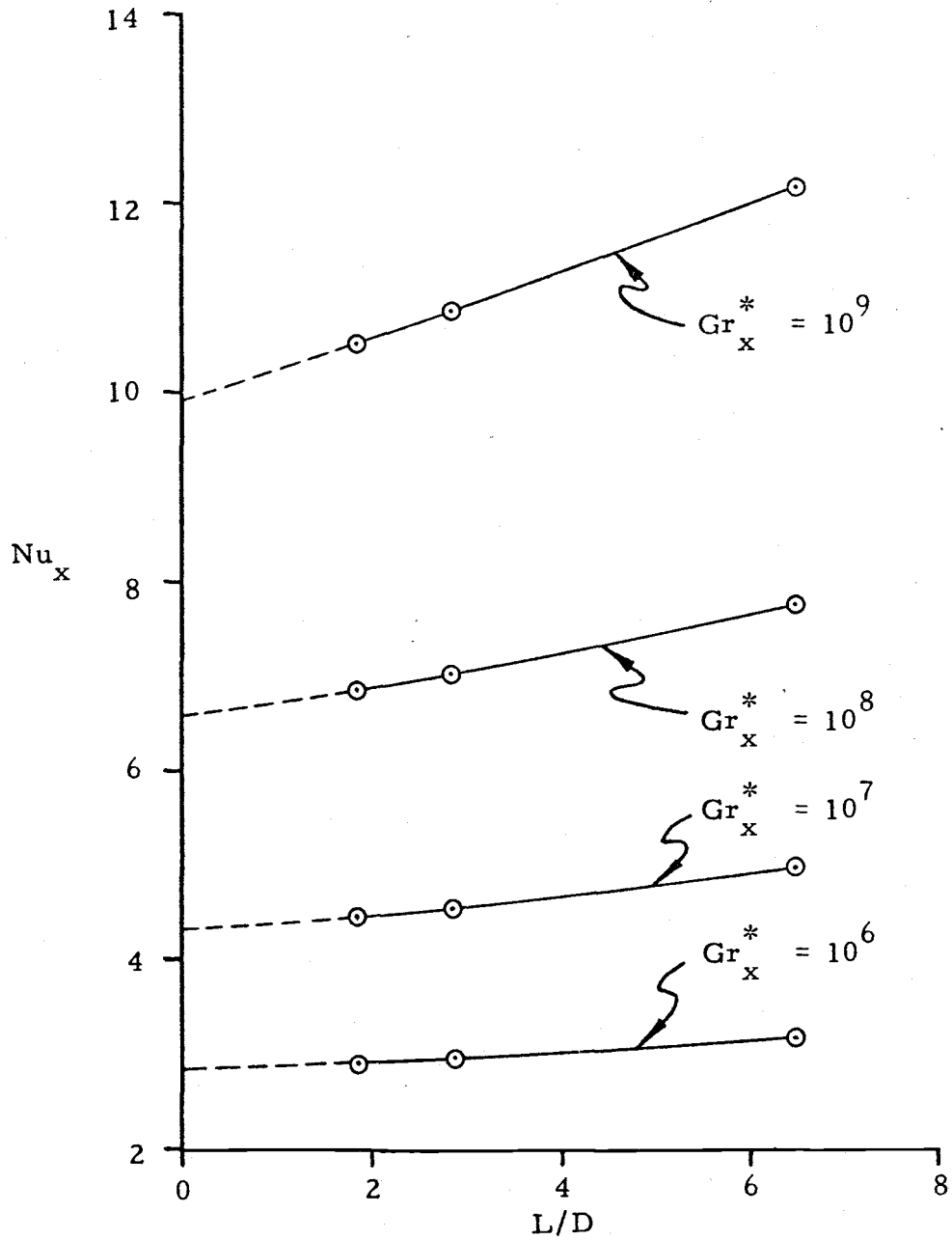


Figure F4.5. Plot to determine Nu_x at $L/D = 0$ for various Gr_x^* .

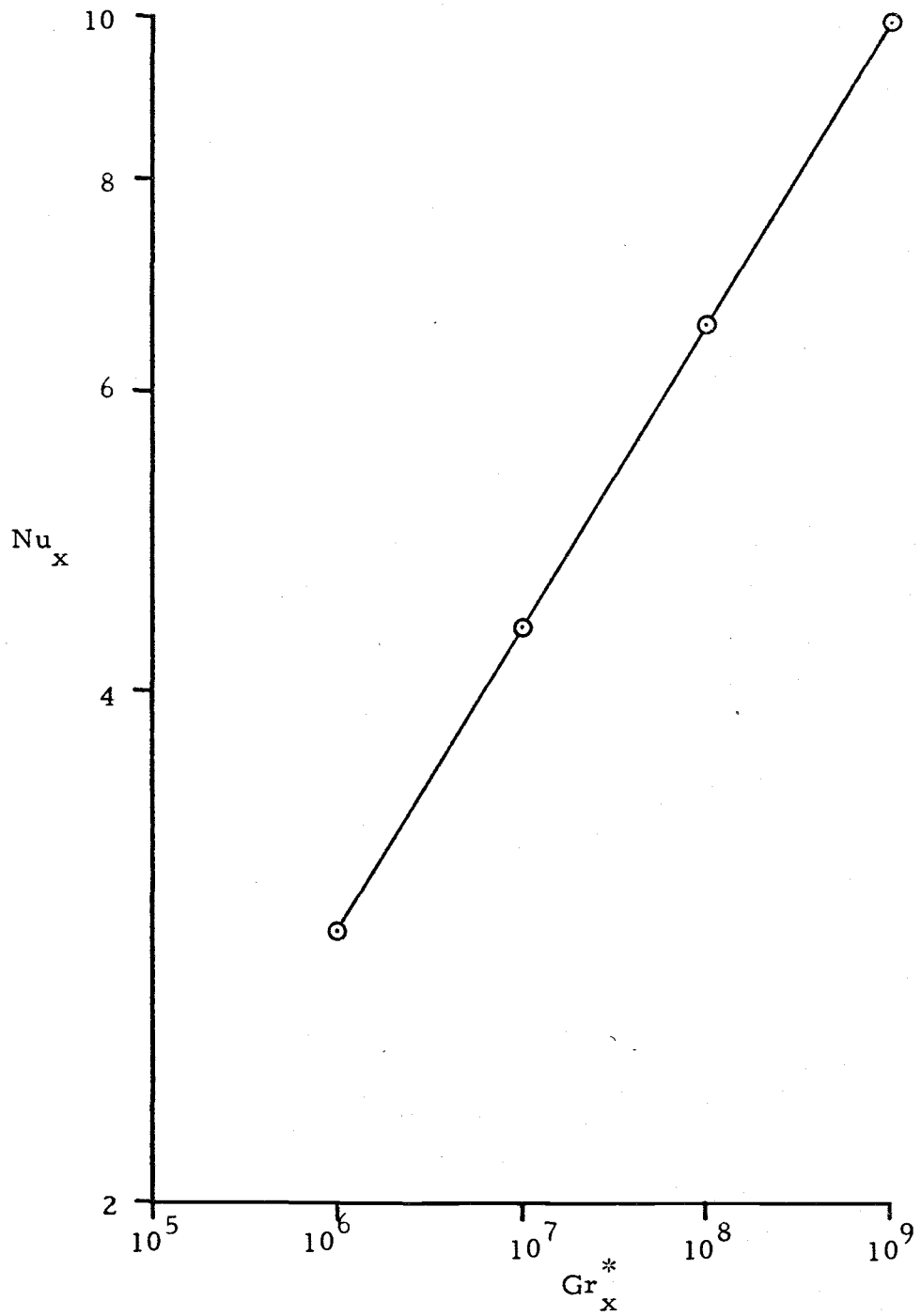


Figure F4.6. Plot of intercepts to determine equation of extrapolation to flat plate.

since it is formulated by extrapolation of the cylinder data.

Equation E4. 5 represents the result that may have been achieved for a flat plate had the same design considerations, techniques, and procedures been used as were done with the cylinders. With a similar heater design as incorporated for the cylinders, Colwell (28) measured the heat transfer from a flat plate using the same instrumentation as was employed in this work. His plate was five inches by five inches. More than fifty data points were regressed to obtain the following correlation for local Nusselt number:

$$\text{Nu}_x = 0.230 (\text{Gr}_x^*)^{0.180} \quad (\text{E4. 6})$$

Comparing equation E4. 5 to E4. 6 it is evident that a significant level of consistency exists in the heat transfer results for the cylinders. Deviation of equation E4. 5 from Julian's (11) result for a vertical uniformly heated flat plate are less than ten percent over the Grashof number range of interest. This indicates that the results for the cylinders are probably not disturbed by any gross systematic errors inherent in the equipment or elsewhere. Agreement with the analytical solution of Chang et al. (9), is also quite good, especially at large Grashof numbers.

The only available information in the literature dealing with constant heat flux vertical cylinders was that of Nagendra et al. (25). His equations for Nusselt number based on diameter can be converted

to express local Nusselt number. This conversion is presented in the appendix, section A. 1. The results of the conversion are (for $Pr = 0.023$)

$$Nu_x = 0.21 (Gr_x^*)^{0.20} \quad \text{; short cylinders}$$

and

$$Nu_x = 0.44 (Gr_x^*)^{0.14} \left(\frac{L}{D}\right)^{0.30} \quad \text{: long cylinders}$$

Note that the result for short cylinders shows no curvature dependence. This result is meant to be satisfactory for flat plates. For short cylinders, characterized by $Ra_D \frac{D}{L} > 10^4$, this equation should be accurate to within eight percent; i. e., such cylinders very nearly represent flat plates. It must be recognized that Ra_D is based on $(T_w - T_\infty)$ and not on $\frac{qL}{k}$ as is the modified Rayleigh number, Ra_D^* .

The local Nusselt number for long cylinders, characterized by $0.05 < Ra_D \frac{D}{L} < 10^4$, is observed to be curvature dependent, i. e., as diameter decreased Nusselt number increased as expected. However, in comparing values of Nu_x from this equation to experimental values, it is apparent that the results of Nagendra tend to over-predict the effect of curvature. The consequence of this is that Nusselt numbers predicted by the analytical results are much higher than experimental values.

A summary of the heat transfer results reported by other authors is presented in Table T4.2. The extrapolation of this work to the flat plate result is also presented for comparison. In Colwell's (28) work, Ar is the aspect ratio associated with a channel. It is the height of the channel divided by the spacing between the opposed plates. The result is for the case of one wall heated and the other wall insulated while the plates are at a fairly wide spacing. All other results are for a single vertical plate. In Figure F4.7 some of these correlations are plotted for comparison. In Figure F4.8 plots of the regressions for the three cylinders (equation E4.1) are drawn and compared to other results.

Table T4.2. Summary of heat transfer correlations for uniform flux flat plates.

Sparrow and Gregg (7)	:	$Nu_x = 0.161 (Gr_x^*)^{0.20}$	Pr = 0.023 Analytical
Chang <u>et al.</u> (9)	:	$Nu_x = 0.157 (Gr_x^*)^{0.20}$	Pr = 0.023 Analytical
Nagendra <u>et al.</u> (25)	:	$Nu_x = 0.208 (Gr_x^*)^{0.20}$	Pr = 0.023 Analytical
Julian (11)	:	$Nu_x = 0.196 (Gr_x^*)^{0.188}$	Pr = 0.022 Experimental
Colwell (28)	:	$Nu_x = 0.203 (Gr_x^*)^{0.181}$	Pr = 0.023 Ar = 2 Experimental
Colwell (28)	:	$Nu_x = 0.230 (Gr_x^*)^{0.180}$	Pr = 0.023 Experimental
This work	:	$Nu_x = 0.232 (Gr_x^*)^{0.181}$	Pr = 0.023 Experimental Extrapolation

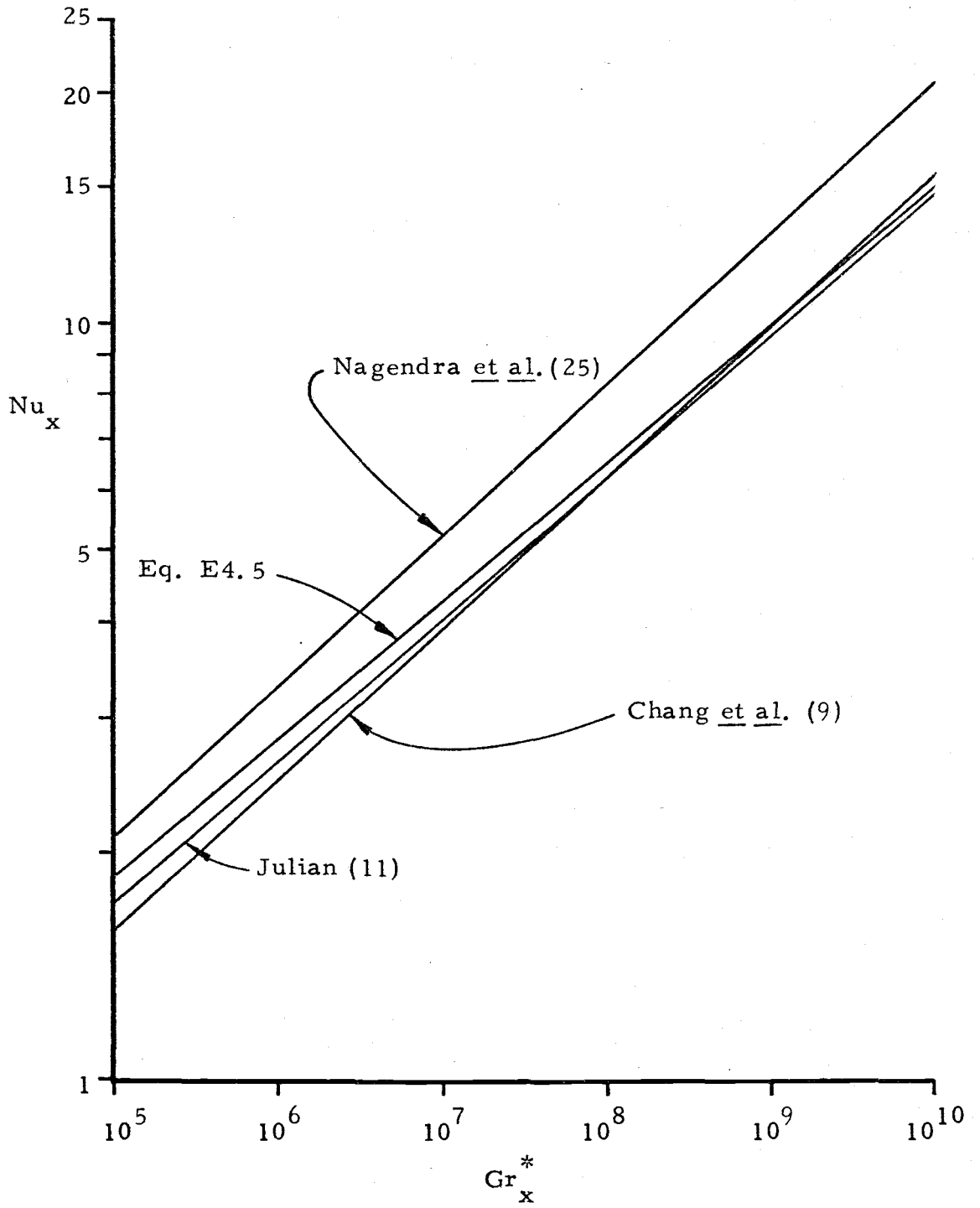


Figure F4.7. Plot of results for uniformly heated vertical flat plates.

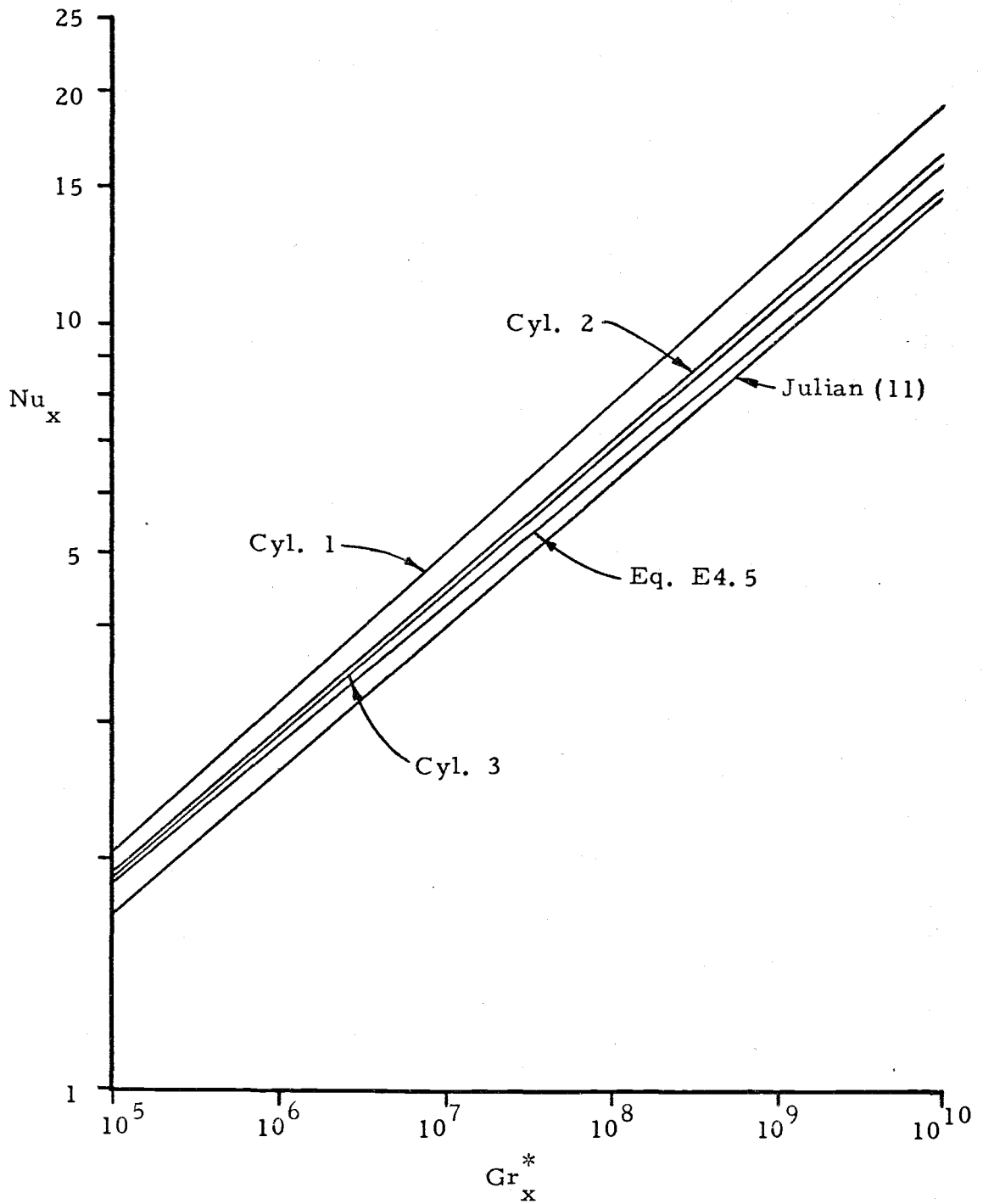


Figure F4.8. Plot of regression equations for cylinders 1, 2, and 3 compared to equation E4.5 and the results of Julian (11).

V. DIMENSIONLESS TEMPERATURE

In order to apply the results of this study to the design of heat transfer elements it is of major importance to be able to determine the temperature of the fluid as a function of axial and radial position. Knowledge of the Nusselt number as a function of Grashof number will provide the surface temperature if the ambient fluid temperature is known. However, to obtain temperatures at positions away from the surface one requires more information. This can be acquired from the dimensionless temperature profiles.

The dimensionless temperature profiles are presented here in terms of θ as a function of η , these being the similarity parameters suggested by Sparrow and Gregg (7). The defining equations for these variables are

$$\theta = \frac{k}{qx} (T - T_{\infty}) \left(\frac{Gr_x^*}{5} \right)^{0.20} \quad (E5.1)$$

and

$$\eta = \frac{r}{x} \left(\frac{Gr_x^*}{5} \right)^{0.20} \quad (E5.2)$$

Many of the results presented in the literature are given as ϕ vs. η where ϕ is defined by $(T - T_{\infty}) / (T_w - T_{\infty})$. Without knowledge of the Nusselt number it would not be possible to calculate absolute values of ΔT from such results. This calculation is possible with the results presented in terms of θ as defined by equation E5.1. Comparison of

the present results to results of others has required the conversion of ϕ to the θ coordinate. The method of the conversion is presented in the appendix, section A. 2.

The dimensionless profiles are presented in Figures F5. 1, F5. 2, and F5. 3 for cylinders 1, 2, and 3, respectively. It may be observed that all but a few points fall below the experimental results of Colwell (28) for a single heated vertical plate. The analytical results of Chang et al. (9), also lies above the experimental results of the cylinders except for the larger values of Grashof numbers corresponding to cylinders 2 and 3. Such behavior would be expected because the effect of curvature is to transfer a given heat flux with a smaller temperature difference than would exist for a flat plate.

According to the results of Sparrow and Gregg (2) the dimensionless profiles should approach that of a flat plate as Grashof number increases. This is certainly a well established trend with cylinders 2 and 3. The profiles for larger Grashof numbers lie closer to the solution for the flat plate. The data for cylinder 1 do not show any such trend, however. After four profiles had been computed for cylinder 1 (for various Grashof numbers) and the plots were observed to be virtually independent of Grashof number, three more profiles were computed to determine if the original results were particular to the sampling of the data. As can be seen on the graph, all seven profiles are nearly coincident. Therefore, this behavior

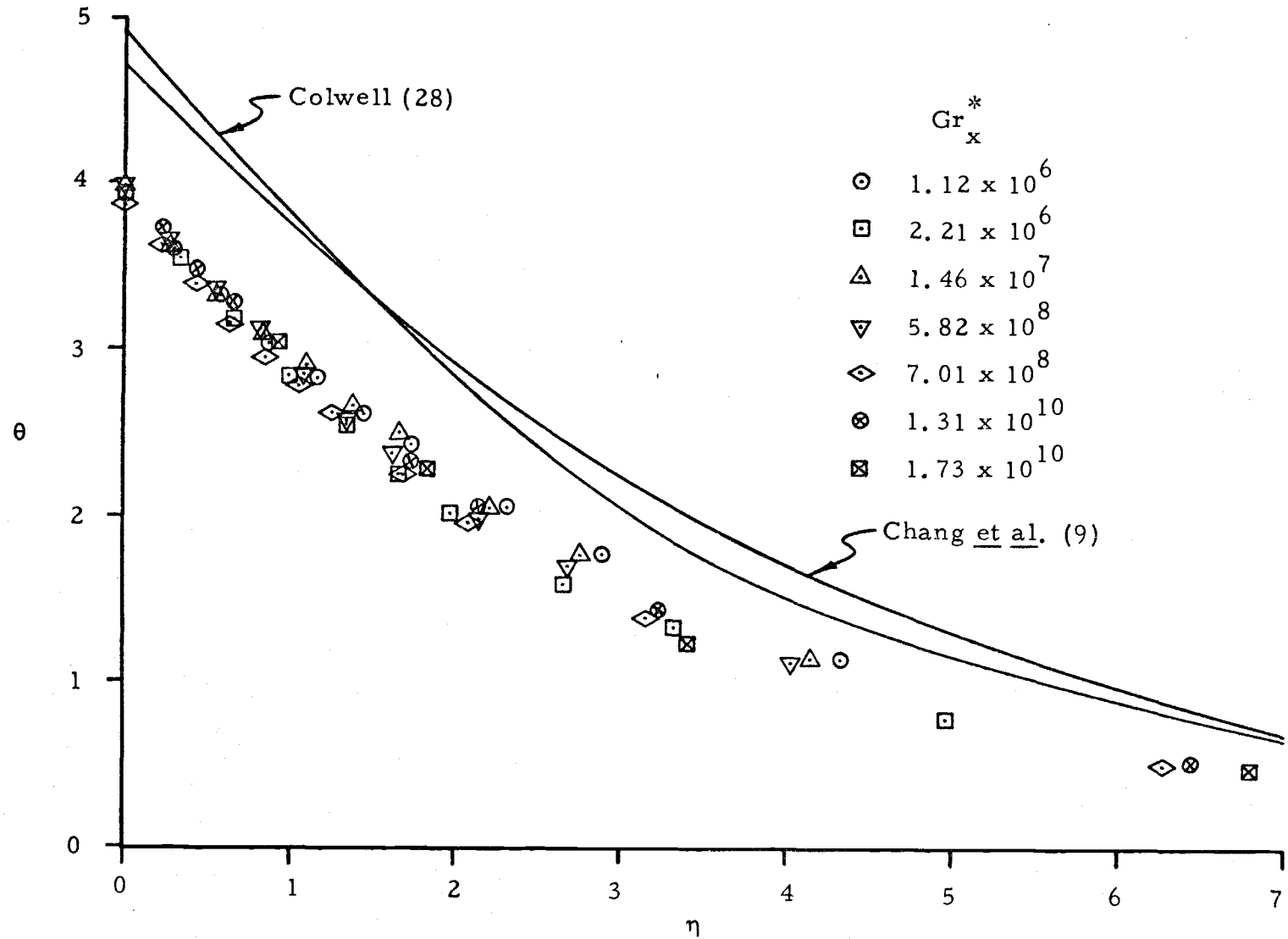


Figure F5.1. Dimensionless temperature; cylinder 1.

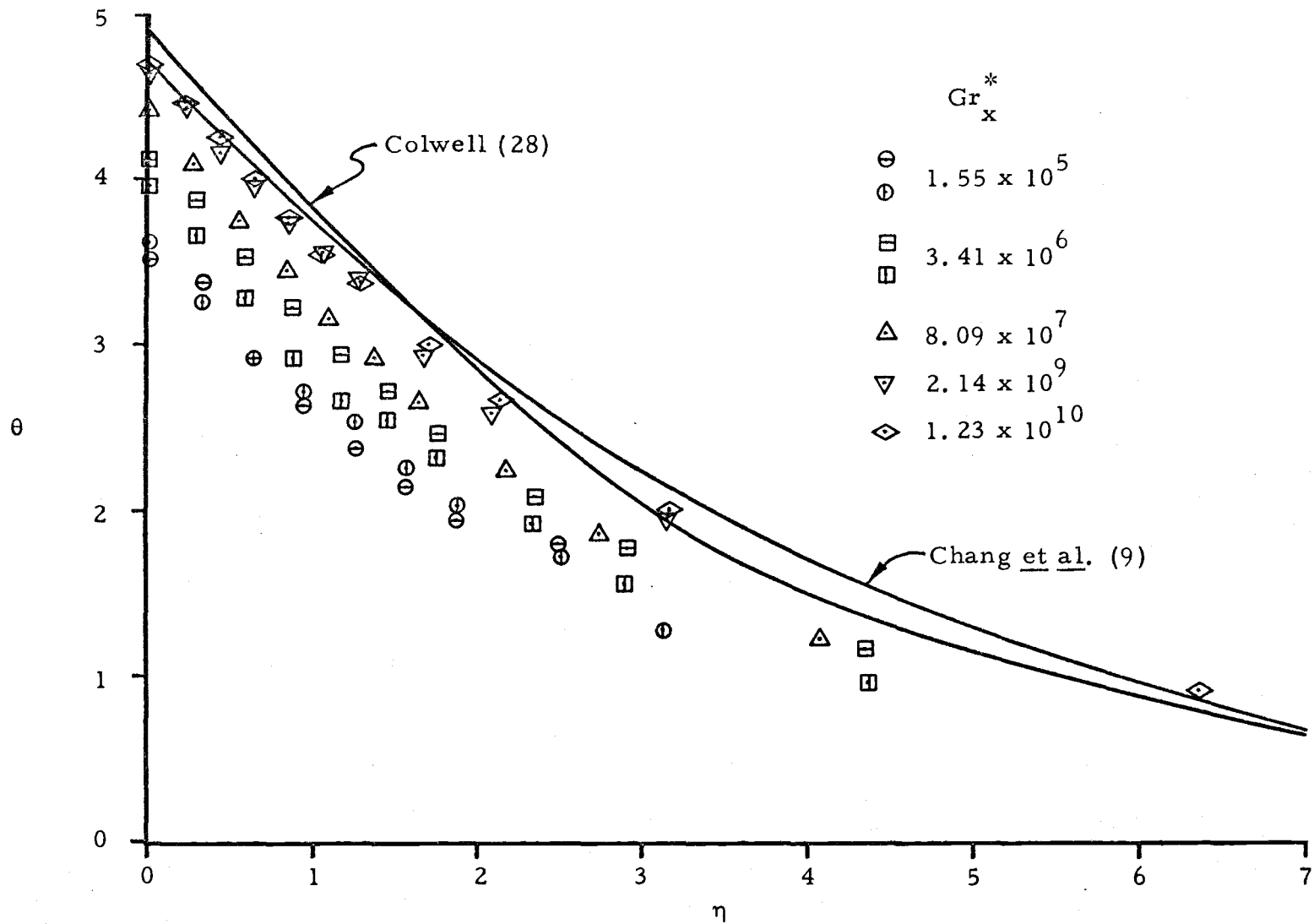


Figure F5.2. Dimensionless temperature; cylinder 2.

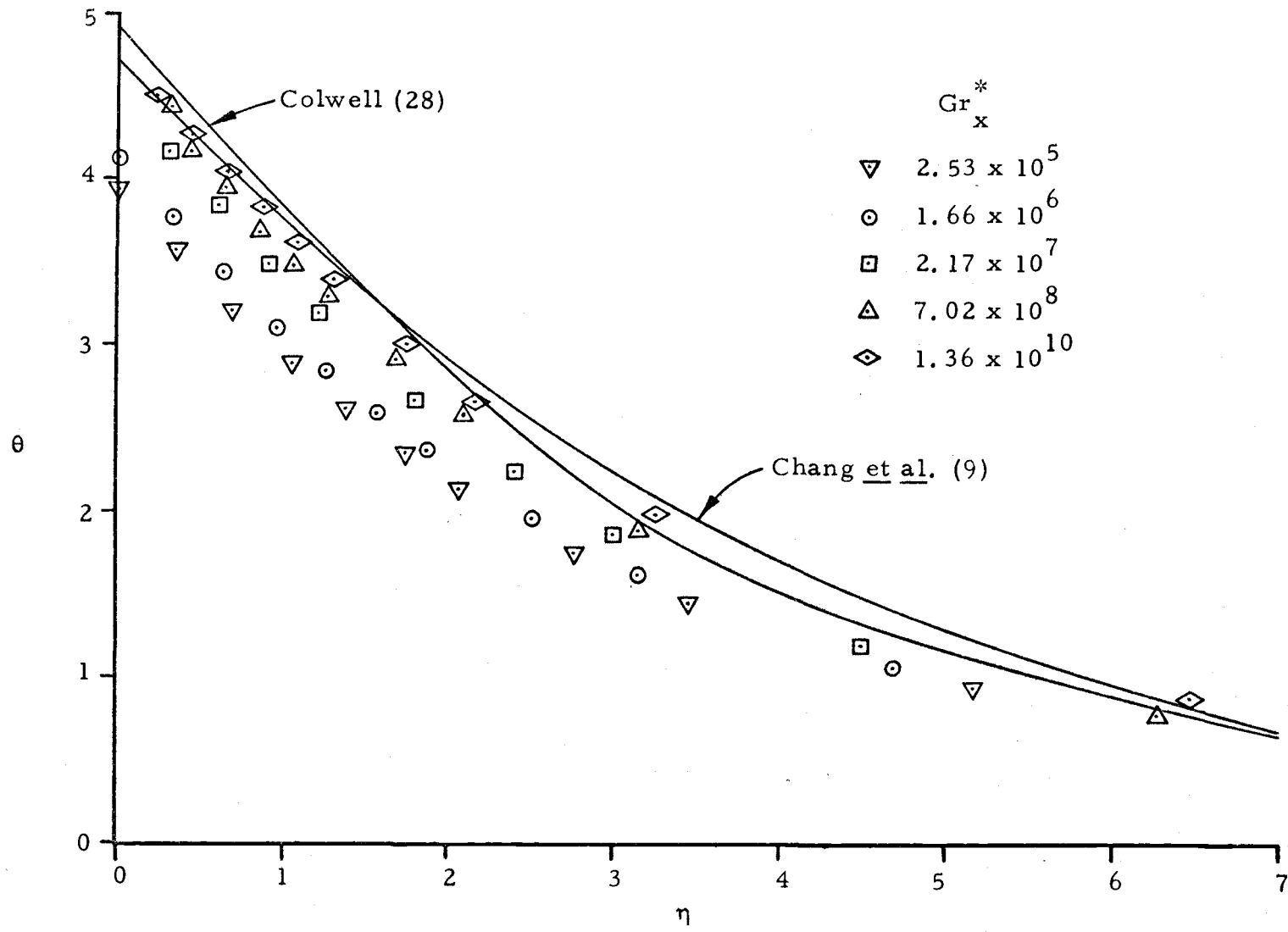


Figure F5.3. Dimensionless temperature; cylinder 3.

is apparently characteristic of the small cylinder.

The particular behavior observed on the dimensionless temperature profiles is not explainable without a significant amount of conjecture. One may suppose at first glance that the data from the two larger cylinders includes significant random scatter. A closer observation reveals, however, that the individual profiles are, indeed, quite smooth. For cylinder 2, two profiles were obtained for the two lower Grashof numbers. While the pairs of profiles are seen to differ, the total variation at the intercept ($\eta = 0$) is four percent for $Gr_x^* = 3.41 \times 10^6$.

Step errors in the profiles could result from taking apparent surface temperature readings with the probe shaft either too close or too far from the surface. If the probe shaft is too close to the surface a true surface temperature is obtained, but the probe shaft is deflected. When the probe is moved away from the surface the first radial increment is in error by the amount of deflection. While all the succeeding intervals are evenly spaced, the entire profile becomes displaced to the right, i. e., to larger values of η . For cylinder 2 and $Gr_x^* = 1.55 \times 10^5$ the profile originating from the lower intercept seems to be influenced by this problem.

If the probe tip were not in contact with the surface the measurement of surface temperature would certainly be in error. The effect of this on the temperature profile is to displace it to the left, i. e., to

smaller values of η and θ . (If ΔT is small by error, θ will be small by the same error.) This may have been the case for cylinder 2 and $Gr_x^* = 3.41 \times 10^6$. If the lower profile were set to the right by an amount $\Delta\eta = 0.20$ then the two profiles would nearly coincide.

Another source of step error would be careless axial location of the probe tip.

Even though many sources of potential error do exist, it would be unreasonable to assume that the apparent Grashof number trend observable for cylinders 2 and 3 would be a result of random errors to which these step errors are included. Instead, one must assume that the data are sound and from that point speculate about the possible cause of the behavior.

Comparing the profiles of cylinder 2 to those of cylinder 3, one observes that for large Grashof number the profiles are nearly coincident. As Grashof number decreases the deviation between the profiles increases with the profiles of cylinder 2 falling increasingly lower than those of cylinder 3. This comparison might be expected because of the difference in curvature of the two cylinders. It may be anticipated that this trend would continue to include cylinder 1, but this is obviously not the case. While all the profiles of cylinder 1 are relatively low they exhibit no Grashof number trend. In other words, there is apparent similarity at the larger curvature. The only logical explanation for this is that cylinder 1 exists within a

separate heat transfer regime. Nagendra et al. (25), expressed a dividing line between short and long cylinders at $Ra_D \frac{D}{L} = 10^4$,

where

$$Ra_D = \frac{\beta g}{\nu} D^3 (\overline{T_w - T_\infty}) Pr$$

This parameter was calculated for cylinders 1, 2, and 3 and found to be $9.1 \times 10^2 \overline{\Delta T}$, $2.5 \times 10^4 \overline{\Delta T}$, and $1.5 \times 10^5 \overline{\Delta T}$, respectively. Values of $\overline{\Delta T}$ were on the order of $5^\circ F$ to $15^\circ F$ for cylinders 2 and 3 and $3.5^\circ F$ to $12^\circ F$ for cylinder 1. Even at the highest heat rate, cylinder 1 could still be considered to be in the category of long cylinders while under no conditions do cylinders 2 and 3 fall into this category. Perhaps, in the regime of short cylinders (considered to be equivalent to flat plates by Nagendra) curvature has a disrupting effect on similarity while in the regime of long cylinders similarity tends to be more characteristic of the heat transfer. Although the subject of similarity of temperature profiles is not discussed by Nagendra, the present results do lend some credence to the classification scheme established by those authors. Certainly, a greater variety of cylinder diameters would have to be considered before any valid conclusions could be established that would characterize the results.

VI. CONCLUSIONS

As a result of the experimental investigation it has been determined that there is a definite influence of curvature upon the natural convection heat transfer from a vertical surface to mercury. If all parameters are held constant, the effect of increasing the curvature is to increase the Nusselt number, i. e., the heat transfer. For the range of curvatures examined the influence is small but certainly not negligible. A literature search provided only one paper concerned with a constant heat flux vertical cylinder. The analytical solution indicates a much greater effect of curvature upon the heat transfer than is observed experimentally.

The results that have been presented here should be repeatable if the same apparatus, procedures and techniques are employed. Errors were evidently within acceptable experimental limits. However it is apparent from comparison of the present results to results of other authors that the outcome of the experimental or analytical efforts can differ by significant amounts. Such discrepancies can most likely be attributed to the peculiar characteristics of the experimental system or the approach to the problem.

In retrospect, the final results would benefit by the inclusion of data from more than three cylinders. Interpolation of the data using the generalized equation explicit in $\frac{D}{L}$ should provide

satisfactory heat transfer information. However, the variation of results with diameter is not well defined and extrapolation of the data should be avoided. The range of $\frac{D}{L}$ for which the results are applicable is 0.15 to 0.55.

An experimental investigation involving a greater number of cylinders with a wider variety of diameters would increase the $\frac{D}{L}$ range. Also, the effect of curvature would be better defined, thus allowing some extrapolation.

BIBLIOGRAPHY

1. Schmidt, E. and W. Beckmann. Tech. Mech. u. Thermodynam., 1. 1-24, (1930).
2. Saunders, O. A. Natural Convection in Liquids, Proc. of the Royal Society of London, A 172, 55-71, (1939).
3. Eckert, E. Introduction to the Transfer of Heat and Mass, 1st Ed., 158-162, McGraw-Hill, New York, N. Y., (1950).
4. Ostrach, S. An Analysis of Laminar Free Convection Flow and Heat Transfer About a Flat Plate Parallel to the Direction of the Generating Body Force, NACA TR 1111, (1953).
5. Sparrow, E. Laminar Free Convection on a Vertical Plate with Prescribed Non-Uniform Wall Heat Flux or Prescribed Non-Uniform Wall Temperature, NACA TN 3508, (1955).
6. Sparrow, E. and J. Gregg. Details of Exact Low Prandtl Number Boundary Layer Solutions For Forced and For Free Convection, NASA MEMO 2-27-59 E., (1959).
7. Sparrow, E. and J. Gregg. Laminar Free Convection From a Vertical Plate with Uniform Surface Heat Flux, Trans. ASME, 78, 435-440, (1956).
8. Gebhart, B. Heat Transfer, 1st Ed., Chpt. 8, McGraw-Hill, New York, N. Y., (1961).
9. Chang, K., R. Akins, L. Burris, S. Bankoff. Free Convection of a Low Prandtl Number Fluid in Contact With a Uniformly Heated Vertical Plate, Argonne National Laboratory - 6835, (1964).
10. Kuiken, H. Free Convection at Low Prandtl Number, Journal of Fluid Mechanics, 37, Pt. 4, 485-498, (1969).
11. Julian, D. and R. Akins. Experimental Investigation of Natural Convection Heat Transfer to Mercury, I and EC Fundamentals, 8, no. 4, 641-646, (November, 1969).

12. White, D. An Experimental Investigation of Natural Convection Heat Transfer from Vertical Flat Plates in Mercury, Ph.D. Thesis, Oregon State University, Corvallis, Oregon, (1971).
13. Mueller, A. Heat Transfer From Wires to Air, Trans. AICHE, 28, (1942).
14. Hill, J. and C. Sleicher. Convective Heat Transfer from Small Cylinders to Mercury, Int. Journal of Heat and Mass Transfer, 12, 1595-1604, (1969).
15. Elenbaas, W. Applied Physics, 19, 1148, (1948).
16. Griffiths, E. and A. Davis, The Transmission of Heat by Radiation and Convection, Food Investigation Board, Special Report #9, Dept. of Scientific and Industrial Research, Gt. Britain, (1922).
17. McAdams, W. Heat Transmission, 1st ed., 244, McGraw-Hill, New York, N. Y., (1932).
18. Carne, J. Heat Loss by Natural Convection from Vertical Cylinders, Philosophical Magazine Journal of Science, Series 7, 24, 634-653, (1937).
19. Elenbaas, W. The Dissipation of Heat by Free Convection, Physics 9, 665-672, (1942).
20. Touloukian, Y., G. Hawkins and M. Jakob. Heat Transfer by Free Convection from Vertical Surfaces to Liquids, Trans. ASME, 70, 13-18, (1948).
21. Sparrow, E. and J. Gregg. Laminar Free Convection Heat Transfer from the Outer Surface of a Vertical Circular Cylinder, Trans. ASME, 78, 1823-1829, (1956).
22. Millsaps, K. and K. Pohlhausen. The Laminar Free Convection Heat Transfer from the Surfaces of a Vertical Circular Cylinder, Journal of the Aeronautical Sciences, 23, 381, (1956).

23. Millsaps, K. and K. Pohlhausen. The Laminar Free Convection Heat Transfer from the Outer Surface of a Vertical Circular Cylinder, *Journal of the Aeronautical Sciences*, 25, 357-360, (1958).
24. Nagendra, H., M. Tirunaryanan and A. Ramachandran. Free Convection Heat Transfer from Vertical Cylinders and Wires, *Chemical Engr. Science*, 24, 1491-1495, (1969).
25. Nagendra, H., M. Tirunaryanan and A. Ramachandran. Laminar Free Convection from Vertical Cylinders with Uniform Heat Flux, *Trans. ASME, Journal of Heat Transfer*, 92, 191-194, (Feb., 1970).
26. Powell, R. and R. Tye. The Thermal and Electrical Conductivity of Liquid Mercury, *Int. Developments in Heat Transfer*, ASME, 1961.
27. Lyon, R., (ed.). *Liquid Metals Handbook*, 2nd ed., Washington, D. C., U.S. Govt. Printing Office, (1952).
28. Colwell, R. Experimental Investigation of Natural Convection of Mercury in an Open, Uniformly Heated, Vertical Channel, Ph. D. Thesis, Oregon State University, Corvallis, Oregon, (1973).

APPENDICES

APPENDIX A. 1

The Conversion of the Averaged Heat Transfer Correlations
Developed by Nagendra et al. (25), to Local Correlations

Short Cylinders

Nagendra's result for short cylinders is

$$\text{Nu}_D = 0.55 \left(\text{Gr}_D^* \cdot \text{Pr} \cdot \frac{D}{L} \right)^{0.20}$$

where short cylinders are characterized by $\text{Ra}_D \cdot \frac{D}{L} > 10^4$. A local correlation must be determined that will satisfy this result when integrated over the length, L , of the surface. Assume that such a correlation is

$$\frac{h_x x}{k} = C \left(\text{Gr}_x^* \cdot \text{Pr} \right)^{0.20}$$

Allow the Grashof number to be written as the product $S \cdot x^4$, where

$$S = \frac{\beta g q}{2 \nu k}$$

Substituting and solving for h_x gives

$$h_x = Ck \left(S \cdot \text{Pr} \right)^{0.20} x^{-0.20}$$

Define the average film coefficient by

$$h_m = \frac{1}{L} \int_0^L h_x dx .$$

Substituting for h_x and integrating yields

$$h_m = C'k (S \cdot Pr)^{0.20} / L^{0.20} ,$$

where $C' = 1.25 \cdot C$.

Multiplying both sides by $\frac{D}{k}$ results in

$$\frac{h_m D}{k} = C' (S \cdot D^4 \cdot Pr \cdot \frac{D}{L})^{0.20} .$$

Noting that $S \cdot D^4$ is Gr_D^* , this reduces to

$$Nu_D = C' (Gr_D^* \cdot Pr \cdot \frac{D}{L})^{0.20}$$

where C' is given by Nagendra as 0.55.

The assumed local correlation, when integrated over the length of the surface, yields the form of Nagendra's result. Therefore, the local correlation representative of Nagendra's averaged results can be interpreted to be

$$Nu_x = 0.44 (Gr_x^* \cdot Pr)^{0.20} ,$$

Long Cylinders

Nagendra's results for long cylinders is

$$\text{Nu}_D = 1.33 \left(\text{Gr}_D^* \cdot \text{Pr} \cdot \frac{D}{L} \right)^{0.14},$$

where long cylinders are classified by $0.05 < \text{Ra}_D \cdot \frac{D}{L} < 10^4$.

To find a local correlation that will yield this result when integrated over L , the same approach is used as for short cylinders. After some trial, the following local correlation is assumed:

$$\frac{h_x}{k} = C \left(\text{Gr}_x^* \text{Pr} \right)^{0.14} \left(\frac{L}{D} \right)^{0.30}.$$

Solving for h_x gives

$$h_x = Ck \left(S \cdot \text{Pr} \right)^{0.14} \left(\frac{L}{D} \right)^{0.30} x^{-0.44}.$$

Integrating to obtain h_m results in

$$h_m = C' k \left(S \cdot \text{Pr} \right)^{0.14} \left(\frac{L}{D} \right)^{0.30} L^{-0.44},$$

where $C' = 1.786 \cdot C$.

After multiplying both sides by $\frac{D}{k}$ and rearranging it can be shown that the equation for h_m reduces to

$$\text{Nu}_D = C' \left(\text{Gr}_D^* \cdot \text{Pr} \cdot \frac{D}{L} \right)^{0.14}.$$

which is precisely Nagendra's result. Therefore, it can be interpreted that the local correlation associated with Nagendra's averaged result is

$$\text{Nu}_x = 0.745 (\text{Gr}_x^* \cdot \text{Pr})^{0.14} \left(\frac{L}{D}\right)^{0.30} .$$

APPENDIX A. 2

The Conversion of ϕ to θ

Graphical and tabulated results for dimensionless temperature are typically given in the literature as ϕ vs. η where $\phi = (T - T_{\infty}) / (T_w - T_{\infty})$. The variables could be related by

$$\phi = f(\eta)$$

or

$$\frac{T - T_{\infty}}{T_w - T_{\infty}} = f(\eta)$$

The variable θ is defined by

$$\theta = \frac{k}{qx} (T - T_{\infty}) \left(\frac{Gr_x^*}{5} \right)^{0.20}$$

Substituting for $(T - T_{\infty})$ from above gives

$$\theta = \frac{k}{qx} (T_w - T_{\infty}) f(\eta) \left(\frac{Gr_x^*}{5} \right)^{0.20}$$

Noting that

$$\frac{k (T_w - T_{\infty})}{qx} = \frac{1}{Nu_x}$$

then

$$\theta = \frac{f(\eta)}{Nu_x} \left(\frac{Gr_x^*}{5} \right)^{0.20}$$

For natural convection about a uniformly heated vertical plate, Nu_x is typically given by

$$Nu_x = C (Gr_x^*)^{0.20}$$

Substituting into the expression for θ gives

$$\theta = \frac{f(\eta)}{1.380 \cdot C}$$

Therefore, to convert from ϕ to θ all that is necessary is to have a value of C and to have values of $f(\eta)$ vs. η .